博士論文

論文題目　Analyses of the measles virus inclusion body in muscle and nervous system

（筋肉・神経系における麻疹ウイルス封入体蓄積の影響の解析）

氏　　名　　権　賢貞

Analyses of the measles virus inclusion body in muscle and nervous system

（筋肉・神経系における麻疹ウイルス封入体蓄積の影響の解析）

権　賢貞

CONTENTS

GENERAL INTRODUCTION

Measles virus (MV) is a non-segmented negative-stranded RNA virus, which belongs to genus *Morbillivirus*. Genus *Morbillivirus* is a member of *Paramyxoviridae*, which is composed of a variety of pathogenic viruses to vertebrates. The family *Paramyxoviridae* is further grouped into two subfamilies, the *Pneumovirinae* and the *Paramixovirinae*. The subfamily *Pneumovirinae* contains two genera: genus *Pneumovirus* and *Metaneumovirus*. The subfamily *Pneumovirinae* contains several well-known viruses, such as human respiratory syncytial virus (hRSV) in the genus *Pneumovirus* and Human metapneumovirus (hMPV) in the genus *Metapneumovirus*. Subfamily *Paramyxovirinae* contains five genera: genus *Respirovirus*, *Rubulavirus*, *Avulavirus, Henipavirus* and *Morbillivirus*. Genus *Respirovirus* contains human parainfluenza virus type 1 and type 3 (PIV-1 and PIV-3), sendai virus (SeV) and bovine parainfluenza virus type 3 (BPIV-3). These viruses cause respiratory diseases in their natural host. Genus *Rubulavirus* contains human parainfluenza virus type 2, 4a and 4b (hPIV2/4a/4b), mumps virus (MuV), and simian virus 5 (SV5). Genus *Avulavirus* contains avian paramyxoviruses and newcastle disease virus (NDV). Genus *Henipavirus* contains hendra virus (HeV) and nipah virus (NiV). Genus *Morbillivirus* contains measles virus (MV), rinderpest virus (RPV), canine distemper virus (CDV), peste des petits ruminant's virus (PPRV), phocine distemper virus (PDV), and cetacean morbilliviruses, including dolphin morbillivirus (DMV) and porpoise's morbillivirus (PMV).

The morbilliviruses include pathogenic viruses important in their host species: MV in human, CDV in carnivores, PDV in seals, cetacean morbillivirus in porpoises and dorphins, RPV in ruminants, and PRRV in small ruminants (Griffin 2007). Morbilliviruses share antigenic similarities and causes similar diseases. MV causes an acute infectious respiratory disease seen mainly in children. Persistence of MV develops some complications in the central nervous system (CNS) such as subacute

sclerosing panencephalitis (SSPE). CDV causes gastroenteritis, pneumonitis, conjunctivitis, and encephalitis in young dogs. Persistent infection of CDV leads to old dog encephalitis (ODE) or hard pad disease. The ODE caused by CDV has similar features to SSPE of MV. Immunosuppression is the common feature of morbillivirus infection. The replication of morbilliviruses occurs mainly in lymphoid organs throughout the body and causes severe lymphopenia in acute infection. The CNS infection of morbilliviruses has many questions regarding the mechanisms of virus spread and pathogenesis. The MVs isolated from the CNS of SSPE patients (SSPE viruses) differ from the wild type MV. SSPE viruses are defective in the release of virions from infected cells (Patterson et al. 2001). The neurons and oligodendrocytes is the most frequently infected cells in the brains of SSPE patients, but it is unknown how the viruses invade these cells (Kirk et al. 1991). The viral RNA was detected in the CNS of all SSPE patients, but the detection of viral antigen tended to be difficult when clinical duration of SSPE became longer (Allen et al. 1996). Like the MV, CDV is detected in neurons of ODE patients, and the replication of virus is defective (Axthelm, Krakowka 1998).

Live attenuated vaccines of morbilliviruses are quite effective to induce immune responses to the infection. The vaccines of MV, CDV and RPV were successfully used to prevent the associated diseases. RPV was eradicated from the globe in 2011 through the use of a safe and effective live attenuated vaccine. The incidence of measles and SSPE was dramatically reduced after the vaccines of MV were widely introduced to the world (Campbell et al. 2007). Global mortality of measles has declined by 78% in 2008 relative to 2000 (Dabbagh et al. 2009). Measles elimination has been sustained in WHO Region of the Americas since 2002, and three WHO regions, European, Eastern Mediterranean and Western Pacific, are aiming to eliminate measles by 2015. Nevertheless, measles outbreaks were still reported in recent years: Sub-Saharan Africa in 2009 and Europe in 2011. The cause of serial outbreaks is seemed to be insufficient vaccine coverage. Some studies demonstrated that vaccine-induced immunity declines over time, and that the immunity may be strengthened by

asymptomatic infection (van den Hof et al. 1999, Sonoda, Nakayama 2001). These reoccurrences of measles imply a necessity to develop a new solution to eradicate measles. The reemerging of virus has also been issued in CDV (Bolt et al. 1997, Haas et al. 1997, Gemma et al. 1996). The incidence of CD was also increased in vaccinated dogs since late 1990s, and the epidemic virus phylogenetically formed new clusters separated from the vaccine strains that were developed in 1950s (Gemma et al. 1996, Iwatsuki et al. 1997). CDV has also been expanding its host range in wildlife. CDV caused high mortalities in lions, leopards, and tigers of national parks in Africa and American zoos in the 1990s (Roelke-Parker et al. 1996, Harder et al. 1996). CDV was also identified as a causative agent of epidemic deaths of seals in Lake Baikal from late 1987 to late 1988 (Mamaev et al. 1995). In 2008, CDV infected rhesus monkeys and crab-eating monkeys in China and Japan (Sun et al. 2010, Morikawa et al. 2008). The CDV strain isolated from the infected monkey had an ability to use human receptor (Sakai et al. 2013). These studies suggest that CDV may have a potential to spread to human.

The genomes of morbilliviruses are approximately 16kb in length, and the viruses replicate in the cytoplasm of the host cell. The genomes of morbilliviruses consist of six structural protein genes, encoding nucleocapsid (N) protein, phosphoprotein (P), matrix (M) protein, fusion (F) protein, hemagglutinin (H) protein, and large (L) protein. The P genes encode not only P proteins but also two non-structural proteins, V and C proteins. The viral genomes form ribonucleoproteins (RNPs) by binding with N, P, and L proteins.

H proteins interact with host cell receptors, and F proteins cause virus-cell fusion and cell-cell fusion to facilitate virus entry into cells and viral spread between cells. The H and F proteins are important for determination of viral tropism, and antigens for induction of neutralizing antibodies and immunity against reinfection. The receptors of morbilliviruses are signaling lymphocyte activation molecule (SLAM/CD150), CD46 (membrane cofactor protein, MCP), and PVRL4/nectin-4. H

proteins interact with the immunoglobulin variable (IgV) domain and the immunoglobulin constant domain (IgC) of extracellular region of SLAM (Tatsuo, Ono & Yanagi 2001). The binding of the H protein with SLAM is responsible for lymphotropism and immunosuppression of morbilliviruses (Leonard et al. 2010). CD46 is a cellular receptor for vaccine and laboratory strains of MV, but other morbilliviruses (such as RPV and CDV) are not able to use this receptor. PVRL4/Nectin-4 was recognized as the third receptor for morbilliviruses (Noyce et al. 2011). The use of PVRL4 as a receptor was confirmed in MV and CDV (Noyce et al. 2011, Pratakpiriya et al. 2012). These three receptors cannot explain the neuropathology of morbilliviruses. Therefore, it is considered that the other unidentified receptor should be in CNS.

The viral matrix (M) proteins, localized at the inner layer of plasma membrane of the infected cells and envelope, are involved in virus budding from the infected cells. The M proteins interact with the N proteins and the cytoplasmic tails of H and F proteins. The interactions of M proteins with N,H, and F proteins are important for viral synthesis and assembly (Iwasaki et al. 2009). Hypermutations of M proteins were observed in SSPE cases and responsible for absence of cell-free virus particle (Patterson et al. 2001). Analysis of viral mutations from SSPE patients revealed extensive A-to-I hypermutations implicating participation of ADAR (Adenosine deaminase acting on RNA) (Cattaneo 1994).

The RNP complex containing the RNA genome and the N,P and L proteins, exhibit helical symmetry and initiate intracellular virus replication. The RNP but not naked RNA is a template for transcription and replication. The N proteins encapsidate the virus genomes and form nucleocapsids. The amino terminal 400 amino acid of the N protein (N-CORE) composes the core region of the nucleocapsid. The carboxyl terminal 125 amino acid of the N protein (N-TAIL) is intrinsically disordered and located outside of the core region (Longhi et al. 2003). The L and P proteins constitute viral RNA-dependent RNA polymerase (RdRp). The L proteins have enzymatic activities that are

required for nucleotide polymerization and the capping and polyadenylation of viral mRNAs (Griffin 2007). The P proteins directly interact with N-TAIL and mediate the association of RdRp with nucleocapsids (Harty, Palese 1995).

The N proteins have an ability to migrate into the nucleus but other structural proteins do not. The nuclear location signal (NLS) of N proteins is in N-CORE region and well conserved. The nuclear export signal (NES) of N is located at positions 4-11 in CDV and RPV, and in N-TAIL region of MV (Sato et al. 2006). The nuclear migration of N protein is not necessary for the virus replication because the virus life cycle is undertaken only in cytoplasm of host. However, the nuclear inclusion bodies of MV composed of N proteins and viral RNAs are observed in CDV and MV patients. The meaning of nuclear inclusion bodies has not yet been elucidated, but it was suggested that the accumulation of intranuclear inclusions of MV might be related with the pathogenicity of persistent infection (Robbins 1983). The N-TAIL has been demonstrated to interact various host proteins, including the heat shock protein Hsp72, translation initiation factor eIF3-p40, interferon regulatory factor 3 (IRF-3), FcγRII, cyclophilin B (CypB), and peroxiredoxin 1 (Prdx1) (Zhang et al. 2002, Sato et al. 2007, Servant et al. 2002, Laine et al. 2003, Watanabe et al. 2011, Watanabe et al. 2010). The effect of the binding between the N-tail and host protein was studied in vitro but not in vivo except Hsp72. T Carsillo, et al reported that Hsp72 affected measles virus neurovirulence, and that major histocompatibility complex haplotype determined the effect of Hsp72 (Carsillo et al. 2009, Carsillo et al. 2006).

The P proteins have two functional domains. The P carboxyl terminal domain (PCT) is well conserved and contains all the regions essential for viral transcription. The P amino terminal domain (PNT) is poorly conserved region. All paramyxovirus P proteins form oligomers through heptad sequence repeats in the PCT region (Curran et al. 1995). This oligomerization domains of the SeV P proteins are tetrameric (Tarbouriech et al. 2000). The crystal structure analysis of MV PCT showed

that MV PCT forms a compact bundle of three alpha-helices, and that long cleft between helices α2 and α3 in PCT embeds and induces folding of the N-TAIL (Johansson et al. 2003). The interaction between PCT and N-TAIL is essential for viral RNA synthesis and imparts specificity of the N protein to encapsidate viral, but not cellular RNAs (Longhi et al. 2003). P proteins have also been shown to use and interact with proteins of the host. Serine/threonine phosphorylation of P protein is carried out by cellular kinases, primarily casein kinase II (Das et al. 1995). The interaction of the P protein with ubiquitin-modifying enzyme A20 and STAT1 contributes the immune evasion of virus (Yokota et al. 2008, Devaux et al. 2007).

The C and V proteins are translated from P gene (Bellini et al. 1985). The C protein has 186 amino acids and its reading frame is accessed by alternative translation initiation. The V protein is produced by edition of P mRNA and shares the first 231 amino acids with the P protein. V protein has 68 amino acids zinc-binding cysteine-rich carboxyl terminal domain which is highly conserved in paramyxoviruses (Paterson et al. 1995). The C and V proteins were reported to counteract the IFN signaling. The V protein binds STAT1 and STAT2 and inhibit STAT-inducible transcription of host antiviral genes (Palosaari et al. 2003). The V protein also prevents MDA5- and TLR7/9-mediated IFN inductions (Pfaller, Conzelmann 2008, Childs et al. 2009). The C protein is also seemed to regulate IFN induction, but the direct effect of the C protein on IFN induction has not been shown (Nakatsu et al. 2008). The C protein also participates in the regulation of viral RNA synthesis. C proteins colocalize with RNP complexes, and recombinant MVs lacking C protein are defective in controlling viral RNA synthesis (Nakatsu et al. 2008, Nakatsu et al. 2013).

Transgenic mouse systems have been widely used as tools to analyze the effect of gene expression in vivo that are unable to be reproduced in vitro. The transgenic mice expressing a viral protein are useful in examining its implication in diseases and the interaction between host and the

virus protein in the persistent or asymptomatic infection. For example, the experiment with transgenic mice carrying HTLV-1 genome suggested the involvement of HTLV-1 in chronic arthritis by observing chronic arthritis (Iwakura et al. 1991). Transgenic mice are also well-used to evaluate the pathogenical changes and the effect of antiviral agents in Hepatitis B virus and hepatitis C virus (Perlemuter et al. 2002, Guidotti et al. 1995, Weber et al. 2002). MV or CDV mRNA transcripts and proteins have been detected in bone cells from the patients with Paget`s disease, however, it was controversial whether the MV participated in the development of osteolytic lesions. The analysis of the transgenic mice expressing MV-N protein (MV-N) in osteoclasts showed elevated incidence of Paget`s-like bone lesions (Kurihara et al. 2011).

In Chapter 1, the author generated transgenic mice expressing MV-N under the control of ubiquitous CAG promoter (MV-N mice). The author observed wasting symptom in mice with restricted MV-N expression in muscle tissues. In Chapter 2, the myopathy in MV-N expressing tissues was characterized. The author observed the accumultation of ubiquitin and autophagy-related proteins in MV-N expressing muscle tissues. The alteration of autophagy by MV-N were also observed in vitro. In Chapter 3, the author examined the neurodegenation that occurred in old MV-N mice. The increased MV-N expression and TDP-43 proteinopathy was observed in brains of mice with symptoms. In vitro, the expressing of MV-N induced neurite outgrowth and the upregulation of autophagy by MV-N was also observed. These results imply the effect of the nucleocapsid proteins on myopathy and neurodegeneration in persistent or asymptomatic MV infection.

.

CHAPTER 1

Generation of transgenic mice expressing measles virus nucleocapsid protein

ABSTRACT

Measles virus (MV) forms inclusion bodies in infected tissues regardless of the existence of infectious virion. Main component of the inclusion body is the nucleocapsid protein of MV (MV-N), the most abundant viral protein in infected cells. Although MV inclusion bodies are frequently observed in various tissues histopathologically after severe infection of MV, the function of them is still unknown. The author observed weight loss and wasting in a part of transgenic mice expressing MV-N. Accumulation of MV-N and degenerative myofibers were observed in muscles of these mice. However, the MV-N expression and myopathy were not detected in MV-N mice without wasting symptom. These results implicate MV-N as a potential etiologic factor in myopathy.

INTRODUCTION

Measles virus (MV), a member of the Morbillivirus genus in the Paramyxoviridae family, causes acute febrile infectious disease that remains an important cause of child death in developing countries (Simons et al. 2012). Approximately in 1 in 10,000 cases, the acute infection develops persistent infection, characterized by high frequency of mutations in MV, loss of infectious virions, and development of subacute sclerosing panencephalitis (SSPE) (Bellini et al. 2005).

Implication of persistently infected MV was suspected as a environmental factor for non-neurological diseases, such as Paget`s disease (Kurihara et al. 2011), otosclerosis (Karosi et al. 2005, McKenna, Mills 1989), and Crohn`s disease (Wakefield et al. 1993) by analyses of reverse transcription-PCR (RT-PCR) or immunohistochemistry. In these diseases, the detection rate of MV was higher than that in normal tissues (Kurihara et al. 2011, Kurihara et al. 2000, Kawashima et al. 2000). Kurihara et al. reported that the measles virus nucleocapsid protein (MV-N) induces osteoclasts to exhibit the “Pagetic phenotype” (Kurihara et al. 2000). But, in other diseases, there is no evidence that the presence of MV induces pathological changes.

The genome of MV consist of six structural protein genes, encoding nucleocapsid (N) protein, phosphoprotein (P), matrix (M) protein, fusion (F) protein, hemagglutinin (H) protein, and large (L) protein. The viral genome forms ribonucleoprotein (RNP) by binding with N, P, L protein, and it can be a template for transcription and replication.

All of the MV replication steps are occurred in the cytoplasm. However, MV forms inclusion bodies in the cytoplasm and nuclei of infected tissues. This phenomenom suggests that the formation of MV inclusion bodies is independent of virus replication. In many studies of SSPE cases, intranuclear MV inclusions were observed as the histopathological diagnostic marker and assumed to participate in the pathogenicity (Lewandowska et al. 2001, Garg 2008). The N protein, which

composes the MV inclusion bodies, is the only MV protein distributed in both cytoplasm and nucleus (Giraudon, Ch & Wild 1984). Thus, it is suggested that the N protein may be important for pathogenicity of persistent MV infection.

In this chapter, the author generated transgenic mice expressing N protein (MV-N mice) ubiquitously to assess pathogenic functions of measles virus N protein (MV-N). A part of MV-N mice showed wasting symptom, and the MV-N expression was well observed in muscle tissues in those mice.

MATERIALS AND METHODS

Generation of MV-N transgenic mice.

To introduce restriction enzyme sites, EcoRI at 5`-end and NotI at 3`-end, the nucleocapsid gene of the HL strain measles virus (MV-N) was obtained from total RNA of MV-infected B95a cells by RT with PrimeScript® Reverse Transcriptase (Takara Bio Inc.), followed by PCR using the following primers: forward primer, 5`-CCCGAATTCATGGCCACACTTTTGAGGAG-3`, and reverse primer, 5`-GAAGCGGCCGCCTAGTCTAGAAGATCTCTGT-3`. The amplified MV-N gene was inserted into the EcoRI/NotI sites of a pCAGGS expression vector containing the chicken beta-actin promoter and cytomegalovirus enhancer, beta-actin intron and bovine globin poly-adenylation signal (Niwa et al, 1991). The resulting plasmid, pCAGGS-MV-N was digested with HindIII and SalI and gel-purified. MV-N transgenic mouse lines were produced by injecting the purified HindIII and SalI fragment into the pronuclei of C57BL/6J×C57BL/6J fertilized eggs. Genotyping was performed by PCR using MV-N-specific primers: forward primer, 5`-AAACCCGGATGTGAGCGGGC-3`, reverse primer, 5`-GTGTCTGGGGCCGTAACCGC-3`. The mouse endogenous gene was amplified by PCR as internal control using the following primers: forward primer, 5`-CAGCTGGGGACCCTGTCTGCG ATT-3`, and revere primer, 5`-GAGCTTTGGTCCCTAGCCTGGGT-3`.

RT-PCR analysis.

Total RNA was extracted from mouse tissues using ISOGEN(Nippon Gene). The extracted RNA was treated with DNase I (Roche), and reverse-transcribed using PrimeScript® Reverse Transcriptase (Takara Bio Inc.) by random hexamer priming or oligo dT priming. The resultant cDNA was PCR-amplified using TaKaRa La Taq polymerase (TaKaRa). For detection of the MV-N mRNA, MV-N specific primers were used as described above. The GAPDH-specific primers (Forward primer,

5`-TGCACCACCAACTGCTTAGC-3`, and reverse primer, 5`- TGGATGCAGGGATGATGTTC-3`) were used as internal control. To ensure that DNA did not contaminate RNA preparations, RNA samples without RT enzyme were used as templates for PCR amplification. PCR amplicons were visualized on agarose gel.

Clinical investigations of MV-N mice

The weight of MV-N mice was mornitored weekly. Peripheral blood was obtained from MV-N mice and wild-type littermates at 8 or 9 weeks of age, then white blood cell number was counted by mixing blood with Turk`s solution.

Histopathological examination.

Tissues of mice were fixed in Mildform® (Wako Pure Chemical Industries), dehydrated, embedded in paraffin, sectioned at 5μm, and stained with haematoxylin and eosin for examination by light microscopy. The following tissues of MV-N mice were examined by light microscopy: brain, heart, lung, spleen, pancreas, intestine, bone (femur and tibia), skeletal muscle (femoral region). Tissues from wild-type littermate and MV-N mice at the same age were used for the comparison.

Immunohistochemical analysis.

Paraffin sections were deparaffinized, rehydrated, and submitted to heat-mediated antigen retrieval in EDTA buffer (1mM, pH 8.0). Endogenous peroxidase activity was blocked by the application of 3% hydrogen peroxide for 10 minutes at room temperature. Blocking was performed with Blockace (Dainihon Pharmaceutics) for 1 hour at room temperature or overnight at 4°C. Before using mouse monoclonal antibody (mAb), blocking of endogenous IgG was carried out with unconjugated AffiniPure Fab fragment donkey anti-mouse IgG (H+L) (Jackson immunoresearch) for 1 hour at room temperature. Sections were then incubated with primary antibody for 1 hour at room

temperature or overnight at 4°C. The following antibodies were used as primary antibodies: anti-MV-N rabbit polyclonal antibody (1:200 dilution). Sections were washed with Tris-buffered saline containing 0.05% Tween 20 (TBS-T), and incubated with biotinylated goat anti-rabbit IgG or horse anti-mouse IgG (Vector Laboratories, 1:750 dilution) for 1 hour at room temperature. The immunoactivity was visualized using the avidin-biotin-peroxidase complex (Vectastain ABC kit, Vector Laboratories) and the 3,3` diaminobenzidine (DAB) treatment.

RESULTS

Generation and characterization of MV-N transgenic mice

To generate mice expressing MV-N in all tissues, MV-N gene was expressed under the control of the CAG promoter. The linear MV-N transgene was microinjected into the pronuclear of fertilized embryos. Approximately 150 mice were derived from microinjected embryos. Four F_0 MV-N mice were identified by PCR genotyping of tail DNA. (Figure 1-2A) All F_0 MV-N mice showed mRNA expression of the MV-N transgene in the tail. (Figure 1-2B)

The wasting symptom seen in two F_0 MV-N mice

All F_0 MV-N mice grew normally initially, but weight of #36 and #39, two out of four F_0 MV-N mice, decreased gradually from 8 weeks of age in comparison with that of their wild-type littermates. (Figure 1-3) The loss of body mass was associated with a hunched posture, ruffled fur and greatly reduced activity. The number of white blood cells was decreased in #36 and #39. (Figure 1-4) At 15 and 17 weeks of age, the symptoms of #36 and #39 progressed rapidly and the mice died. In contrast, the two remaining F_0 MV-N mice (#1 and #2) were non-symptomatic and used for establishment of transgenic lines.

Histopathological changes in MV-N mice with symptom

To determine the cause of weight loss and death in #36 and #39 (MV-N mice with symptom), brain, heart, lung, liver, spleen, pancreas, intestine, bone (femur and tibia) and a skeletal muscle (femoral region) of #36 were examined histopathologically. In pancreas, brain, lung, and bone, no pathological change was observed except mild pulmonary edema. (Figure 1-5A) Spleen showed depletion of leukocyte consistent with leukopenia in peripheral blood. (Figure 1-5B) Degenerative lesions were also seen in all type of muscle, such as enlargement of nuclei in cardiac muscle, muscular

atrophy in smooth and skeletal muscle (Figure 1-6, middle panel) Enlargement of nuclei in cardiac muscle is seen in the patients of dilated cardiomyopathy (Schaper et al. 1991) and likely to be related to the cause of death. Histopathological examination of muscle tissues obtained from offsprings of #1 and #2 mice (MV-N mice without symptom) was also performed to assess whether they had myopathy like #36 and #39. MV-N mice without symptom showed normal morphology. (Figure 1-6)

MV-N expression was restricted to muscle tissue of MV-N mice with symptom.

To find direct relation between MV-N and these lesions, tissues described above were immunostained with anti-MV-N antibody. Obvious MV-N expression was noted in cardiac, smooth, and skeletal muscles of MV-N mice with symptom, but not in spleen, pancreas, brain, lung, and bone, although the MV-N transgene was designed to express ubiquitously. MV-N was partially or rarely observed in pancreas, brain, lung, bone, and spleen. (Figure 1-7) MV-N formed inclusion-like structures in cardiac and skeletal muscles, whereas MV-N expressed homogenously in smooth muscles. (Figure 1-8, middle panel) The author assessed the MV-N expression in MV-N mice without symptom. MV-N expression was not detected in muscle tissues of MV-N mice without symptom. (Figure 1-8, lower panel) Thus, the myopathy seen in MV-N mice with wasting symptom is related to MV-N expression.

DISCUSSION

Transgenic mice expressing viral antigen are valuable models to study the host-pathogen interaction and uncover the pathogenesis of virus in vivo. In this chapter, the author generated MV-N mice and observed the muscle-restricted expression of MV-N and occurrence of myopathy.

MV-N transgene was designed to express ubiquitously by using CAG promoter. However, MV-N expression was detected distinctly in muscle tissues of symptomatic mice (Figure 1-8), while negligible amount of MV-N was seen in most tissues of MV-N mice. (Figure 1-7) The author detected MV-N transcripts in tail tissues of all F_0 mice (Figure 1-2B) and muscle tissues of non-symptomatic mice (data not shown). It is unknown what regulates MV-N transgene expression in vivo, but MV-N expression may be dependent on integration site in genome or posttranscriptional or posttranslational regulation. Altered expressions of viral transgene were already reported. For example, in hepatitis B virus (HBV) transgenic mice, the expression of HBV was inhibited by TNF or IFN-γ (Puro, Schneider 2007, Heise et al. 1999). In human immunodeficiency virus (HIV) type 1-transgenic mice, some microbial infections and host factors induced integrated HIV expression (Equils et al. 2003, Gazzinelli et al. 1996, Doherty et al. 1999). To identify the host factor associated with the expression of MV-N is expected to elucidate the mechanism of MV persistence.

MV-N mice showed degeneration in cardiac muscle as well as skeletal muscle (Figure 1-6). Some metabolic myopathies are associated with cardiomyopathies (Dalakas et al. 2000, Connuck et al. 2008). This implies the possibility that the myopathy by MV-N is occurred by metabolic disturbance. In addition, MV-N formed inclusion body-like dots in cardiac and skeletal muscles, but not in smooth muscles. The similar expression pattern of MV-N between cardiac and skeletal muscles suggests that the mechanism of myopathy by MV-N may have similarities between cardiac and skeletal muscles.

Atrophy of spleen was one of symptoms of wasting MV-N mice, but MV-N was scarcely

detected in spleen. (Figure 1-7B) The leukopenia and spleen atrophy seen in MV-N mice seems to be a secondary symptom of cardiac degeneration or a result of MV-N expressing cell death. Barth syndrome, a severe fatal inherited disorder, is characterized by dilated cardiomyopathy, skeletal myopathy, and neutropenia (Barth et al. 1983). The neutropenia seen in this disorder is due to inhibition of differentiation in hematopoietic stage. If defective metabolism is induced by MV-N in hematopoietic stage, leukopenia could occur without expression of MV-N in blood cells.

To date, there were few studies addressing whether MV participates in myopathy, and no MV antigen was detected in a study of inclusion body myositis (IBM) cases (Chou 1986). The MV-N expressing mice showed myopathies and possibility of myodegeneration due to MV-N. Characterization of the myopathy seen in MV-N mice should promote better understanding of pathological function of MV inclusion body.

FIGURE LEGENDS

Figure 1-1. Generation of MV-N transgenic mice.

The transgene containing CAG promoter and MV-N ORF was microinjected into the pronucleus of fertilized eggs. The blue arrow under the schematic of transgene represents the genotyping PCR product. The eggs were implanted into pseudopregnant mice.

Figure 1-2. Detection of F_0 mice and expression of MV-N transcripts.

(A) PCR-based genotyping of F_0 mice. Mouse tail DNA was used as a template. The PCR product specific for the MV-N gene was obtained from 4 F_0 mice (#36, #39, #1, and #2). The mouse endogenous gene was detected in all mice. The length of the PCR products were 380 bp (MV-N) and 457 bp (mouse endogenous gene). (B) MV-N mRNA expression in mouse tail tissues. Mouse tail tissue was obtained at 4~39 weeks of age. MV-N mRNA was detected in all tail tissues of F_0 mice. GAPDH mRNA was used as internal control. To control DNA contamination, RNA samples without RT enzyme (RT-) were used as template for PCR with GAPDH-specific primers.

Figure 1-3. Weight loss in MV-N mice.

The weight of MV-N mice was compared with their wild-type littermates. Weight loss was observed in #36 and #39 mice (A). The #1 and #2 mice grew normally (B).

Figure 1-4. Leukopenia in mice with wasting symptom

White blood cells (WBC) of MV-N mice were obtained at 8~9 weeks of age. For WBC count, Turk`s solution was used. The number of WBC was standardized with that in wild-type littermates. 3 littermates were used for comparison with each MV-N mice except #2. Each value represents the average ± standard deviation.

Figure 1-5. H&E staining of non-muscle tissues of MV-N mice with symptom.

H&E staining of MV-N mice shows no abnormal pathology in pancreas, brain, lung, and bone except for mild pulmonary edema (A). In spleen, leukocyte depletion was detected in MV-N mice with symptom (B). The scale bar represents 100 μm.

Figure 1-6. H&E staining of muscle tissues of MV-N mice.

Muscles from wild-type mice and MV-N mice without wasting symptom showed normal morphology with H&E staining (upper and lower panel). In MV-N mice with symptom (middle panel), bizarre enlarged nuclei in cardiac muscle (arrows) were increased. The atrophy of smooth muscle fibers and fibrous replacement were observed in intestine of MV-N mice with symptom. In thigh skeletal muscles of MV-N mice with symptom, the size of myofibers of #36 was irregular and decreased relative to wild-type and MV-N mice without symptom. The scale bar represents 50 μm. Inset shows an enlarged view of the boxed region.

Figure 1-7. MV-N immunostaining of non-muscle tissues of MV-N mice with symptom.

MV-N was detected in pancreas of #39 and respiratory epithelium of MV-N mice (A). In spleen, MV-N was detected in perivascular region but not in leukocytes (B). The scale bar represents 100 μm. The enlarged views are shown in the insets.

Figure 1-8. MV-N immunostaining of muscle tissues of MV-N mice.

MV-N was detected in muscle tissues of MV-N mice with symptom (middle panel) but not in wild-type mice (upper panel) and MV-N mice without symptom (lower panel). In MV-N mice with symptom, MV-N formed dot-structure in cardiac muscle and skeletal muscle. Red arrows indicate the MV-N-positive dots. MV-N expressed diffusely in smooth muscle. The scale bar represents 50 μm.

Figure 1-1

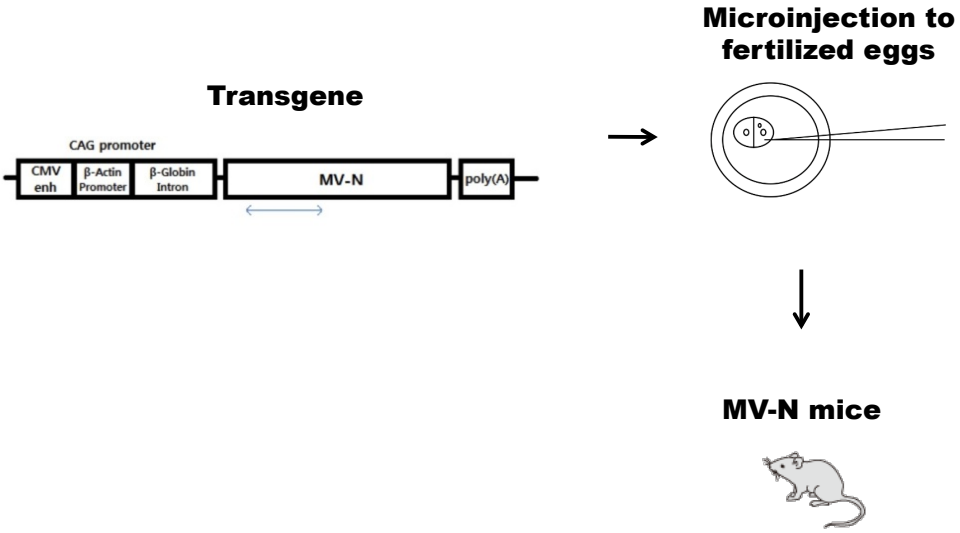
Transgene
CAG promoter
CMV enh
β-Actin Promoter
β-Globin Intron
MV-N
poly(A)
Microinjection to fertilized eggs
MV-N mice

Figure 1-2

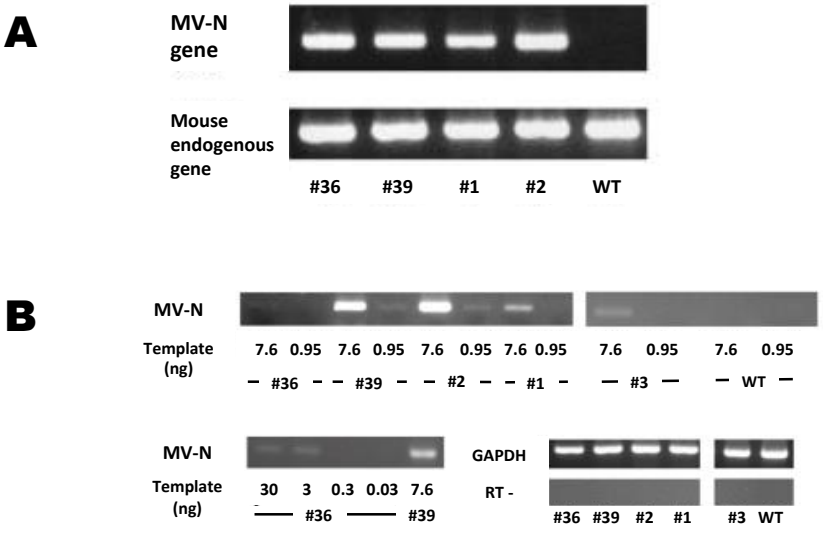
A
MV-N gene
Mouse endogenous gene
#36 #39 #1 #2 WT
B
MV-N
Template (ng)
7.6 0.95 7.6 0.95 7.6 0.95 7.6 0.95 7.6 0.95 7.6 0.95
#36 #39 #2 #1 #3 WT
MV-N
Template (ng)
30 3 0.3 0.03 7.6
#36 #39
GAPDH
RT -
#36 #39 #2 #1 #3 WT

Figure 1-3

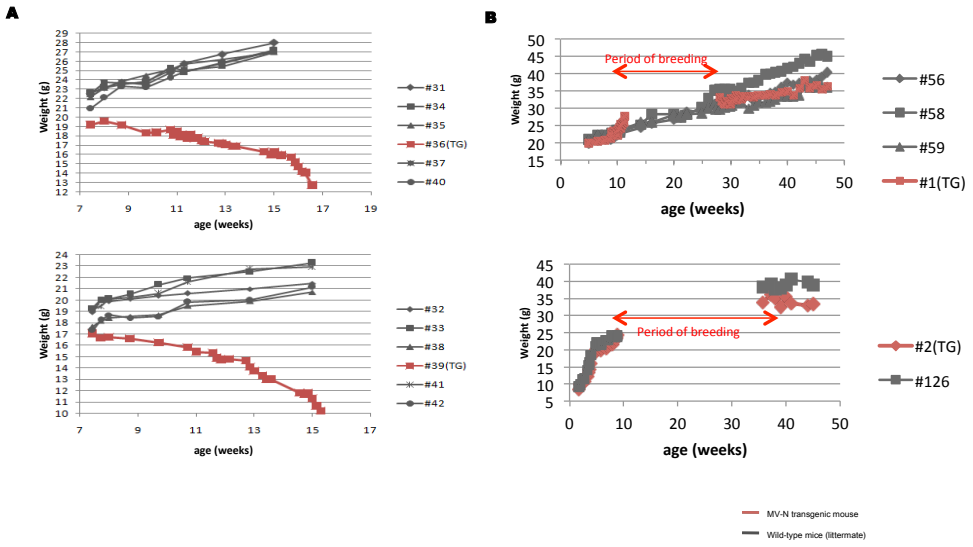
A
Weight (g)
age (weeks)
#31
#34
#35
#36(TG)
#37
#40
#32
#33
#38
#39(TG)
#41
#42
B
Period of breeding
#56
#58
#59
#1(TG)
#2(TG)
#126
MV-N transgenic mouse
Wild-type mice (littermate)

Figure 1-4

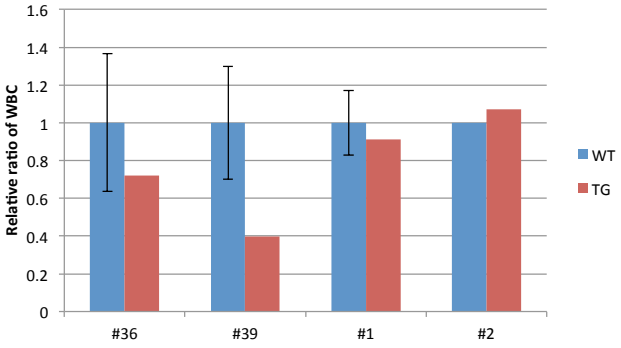

Figure 1-5

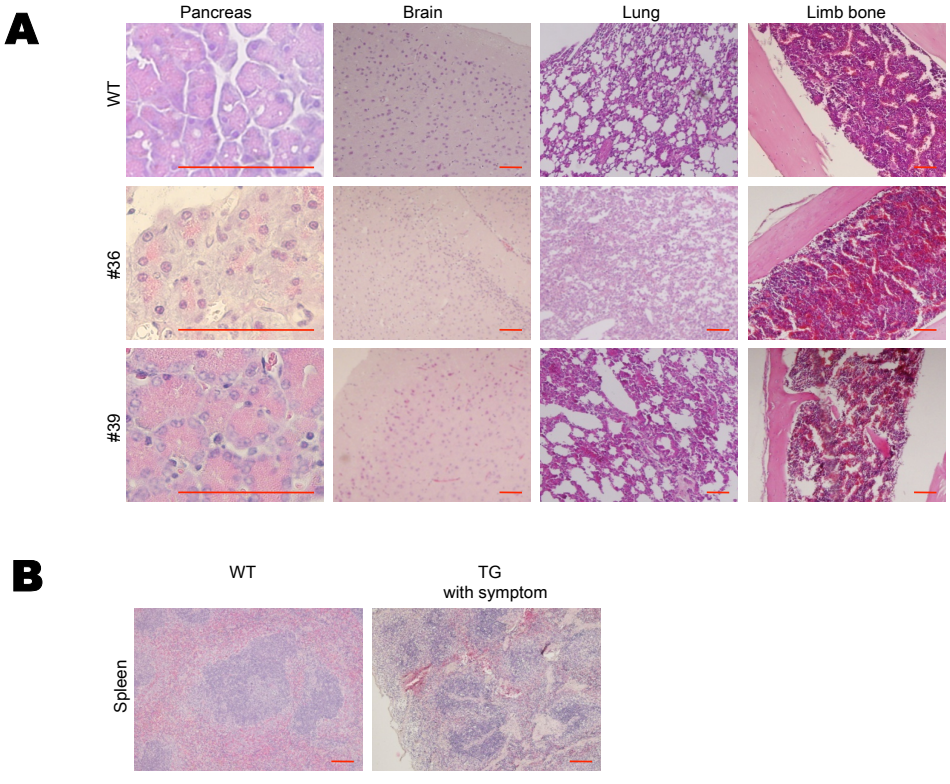
A
Pancreas
Brain
Lung
Limb bone
WT
#36
#39
B
WT
TG
with symptom
Spleen

Figure 1-6

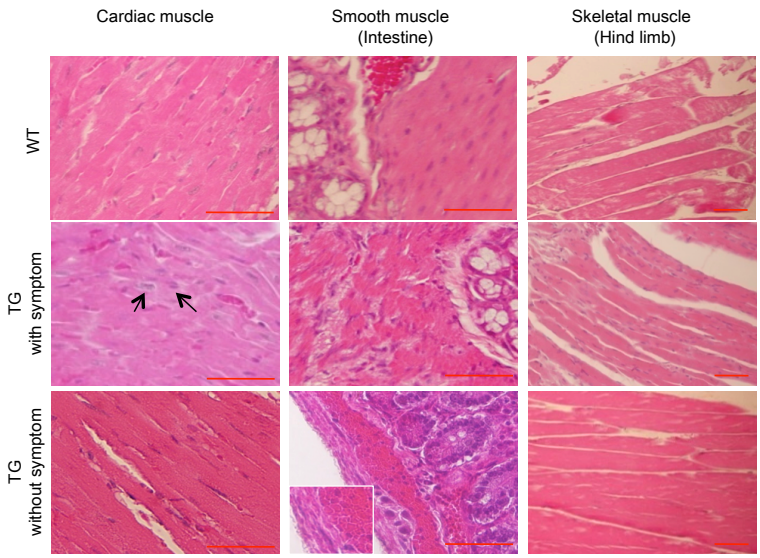
Cardiac muscle
Smooth muscle
(Intestine)
Skeletal muscle
(Hind limb)
WT
TG
with symptom
TG
without symptom

Figure 1-7

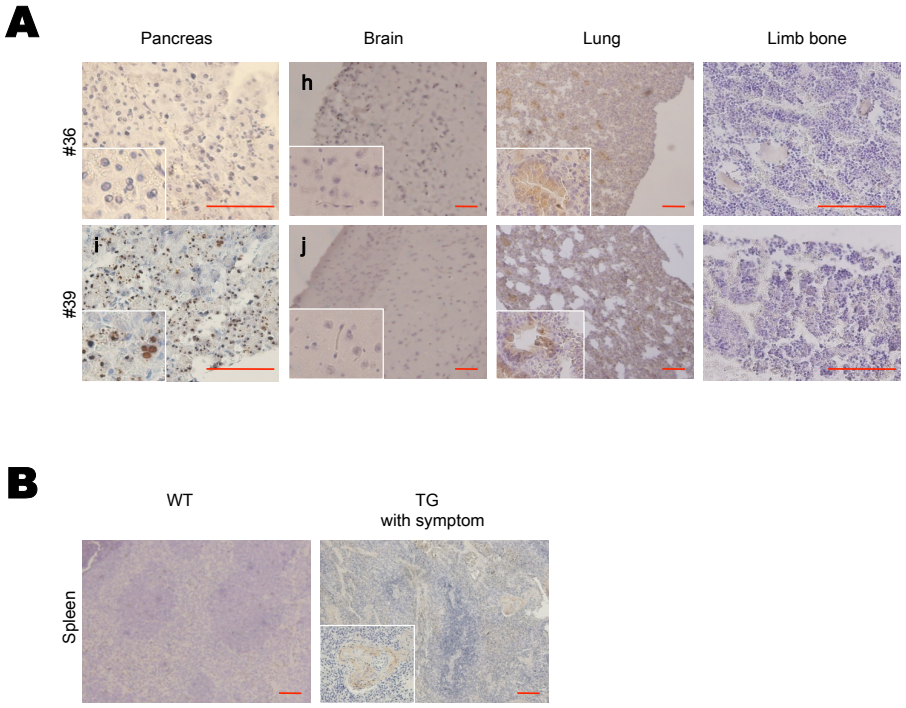
A
Pancreas
Brain
Lung
Limb bone
#36
#39
h
i
j
B
WT
TG
with symptom
Spleen

Figure 1-8

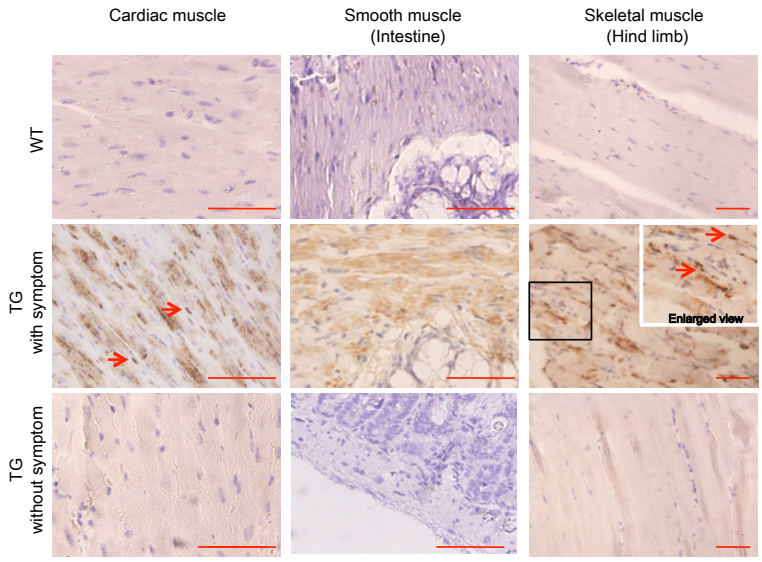
Cardiac muscle
Smooth muscle
(Intestine)
Skeletal muscle
(Hind limb)
WT
TG
with symptom
TG
without symptom
Enlarged view

CHAPTER 2

The effect of measles virus nucleocapsid protein on myopathy

ABSTRACT

Transgenic mice expressing measles virus N protein (MV-N mice) generated by the author showed myopathy. The author characterized the features in detail and found that the pathological feature of the cardiac and skeletal muscle is similar to hereditary inclusion body myopathy (h-IBM). The author also detected accumulation of ubiquitin and autophagy-related proteins in the muscle. In the mouse myoblast cell line C2C12, the author found the MV-N inhibited the myogenic differentiation. The exhaustion of LC3 and increased p62 aggregates were also observed in MV-N expressing C2C12 cells. These results suggested that the MV-N is associated with the myopathy characterized by altered autophagic flux.

INTRODUCTION

Measles virus (MV), a member of the Morbillivirus genus in the Paramyxoviridae family, is an enveloped virus with a nonsegmented negative-strand RNA genome. The MV infection causes acute febrile infectious disease and infrequently develops into neurological disorder such as subacute sclerosing panencephalitis (SSPE). The live measles vaccine became available in the early 1960s, and the vaccine against measles was very effective and reduced the incidence of measles including SSPE worldwide. However, serological studies demonstrated that vaccine-induced immunity wanes over time and is less protective than immunity acquired by natural MV infection (van den Hof et al. 1999, Muller 2001). It was suggested that asymptomatic measles virus infection sustains vaccine-induced immunity (Sonoda, Nakayama 2001, Ozanne, d'Halewyn 1992). MV genome was detected in peripheral blood mononuclear cells (PBMC) of healthy people and various tissue samples obtained from autopsy subjects without MV-related symptoms (Sonoda, Nakayama 2001, Katayama et al. 1998).

Although transmission from asymptomatic infections is seems to be very rare, these asymptomatic MV infections has been suggested to have an association with a lot of diseases such as multiple sclerosis, Paget`s disease, otosclerosis (Kurihara et al. 2011, González-Scarano, Rima 1999, Niedermeyer et al. 2000).

It was debated largely during the 1970s-90s whether paramyxovirus is relevant to myopathy. The microtubular filaments, demonstrated by electron microscopic examination of inclusion body myositis (IBM) patients, resemble helical nucleocapsid protein found in paramyxovirus-infected cells or in brain tissues of SSPE patients (Chou 1967). There have been several reports trying to detect paramyxovirus antigens in IBM patients by immunohistochemistry. However, most of these studies focused on mumps virus and studies trying to detect measles virus were rare. Chou SM demonstrated

that mumps virus but not measles virus was detected in muscle biopsies of 8 IBM patients (Chou 1986).

The autophagy system is a degradative pathway that delivers the portion of cytoplasm, organelles, glycogen, and protein aggregates to the lysosome. After induction of autophagy, isolation membrane or phagophore elongates and subsequently encloses a portion of cytoplasm, which results in the formation of autophagosome, a double-membraned structure. Then, the outer membrane of autophagosome fuses with a lysosome and forms an autolysosome, leading to the degradation of entrapped materials and inner autophagosomal membrane. Amino acids and other small molecules generated by autophagic degradation are reused in cytoplasm. The steps of autophagy involve a set of evolutionarily conserved gene products, the Atg proteins. The ULK/Atg1 kinase complex, the autophagy-specific PI3-kinase complex, and the PI3P effectors are important for the nucleation of the isolation membrane. In elongation step, Atg12- and LC3/Atg8-conjugation systems act as key components. (He, Klionsky 2009) Most of the Atg proteins are observed on isolation membranes during nucleation and elongation steps, but only microtubule-associated protein light chain 3 (LC3/Atg8) attachs to the complete autophagosome. Therefore, the LC3 is used as a marker of the autophagosome. (Mizushima, Yoshimori & Levine 2010)

In normal muscle, autophagosomes are morphologically unremarkable. Autophagic vacuoles have been found in degenerative myofiber of rimmed vacuolar myopathies, such as hereditary inclusion body myopathy (h-IBM) and distal myopathy with rimmed vacuoles (DMRV) (Nishino 2003). The lesions of these myopathies are characterized by muscle loss, protein aggregates, and detection of ubiquitin and p62/SQSTM1 (Sandri 2010b). The characteristics of rimmed vacuolar myopathies appeared in the autophagy-related gene knockout mouse models (Sandri 2010a). These results suggested that impaired function of autophagy may lead to muscle degeneration.

In Chapter 1, the author generated transgenic mice expressing MV-N (MV-N mice) and

observed myopathy in MV-N mice. In this chapter, the author characterized the myopathy of MV-N mice and noticed that myofiber degeneration of MV-N mice had similar features to h-IBM. The author also studied the MV-N function in the inhibition of myogenic differentiation in vitro.

MATERIALS AND METHODS

Immunohistochemical analysis.

Paraffin sections were deparaffinized, rehydrated, and submitted to heat-mediated antigen retrieval in EDTA buffer (1mM, pH 8.0) or citrate buffer (10mM, pH 6.0). Antigen-retrieved sections were processed to immunostaining as described in Chapter 1. The following antibodies were used as primary antibodies: anti-MV-N rabbit polyclonal antibody (1:200 dilution, antigen retrieval in EDTA buffer), anti-ubiquitin (P4D1) mouse mAb (Cell signaling, 1:250 dilution, antigen retrieval in citrate buffer), anti-tau (TAU-5) mouse mAb (Calbiochem, 1:250 dilution, antigen retrieval in citrate buffer), anti-p62 (2c11) mouse mAb (Abnova, 1:200 dilution, antigen retrieval in citrate buffer), anti-LC3A/B rabbit polyclonal antibody (Cell signaling, 1:200 dilution, antigen retrieval in EDTA buffer) Before using mouse monoclonal antibody (mAb), blocking of endogenous IgG was carried out with unconjugated AffiniPure Fab fragment donkey anti-mouse IgG (H+L) (Jackson immunoresearch) for 1 hour at room temperature.

Cell culture and establishment of C2C12 cell line stably expressing MV-N

The mouse myoblast cell line C2C12 was purchased from the Cell Engineering Division of RIKEN BioResource Center (Tsukuba, Ibaraki, Japan) and grown in Dulbecco`s minimal essential medium (DMEM) containing 10% fetal calf serum (FCS). pCAGzc, which is a pCAGGS derivative vector possessing zeocin resistance, was constructed as described previously (Watanabe et al. 2010). The MV-N gene was amplified as described above and inserted into the EcoRI/NotI sites of a pCAGzc to construct the expression plasmid pCAGzc-MV-N. C2C12 cells were transfected with pCAGzc-MV-N using Lipofectamine 2000 (Invitrogen), and selected by use of 300 μg/ml of zeocin (Invivogen). Several zeocin-resistant clones were picked, and MV-N expression was confirmed by

immunofluorescence staining using anti-MV-N rabbit polyclonal antibody. In the same way, another C2C12 cell line carrying an empty vector, pCAGzc, was established as a negative control.

Differentiation of C2C12 cells expressing MV-N or infected with MV

MV-N or pCAGzc-expressing C2C12 clones were seeded in a 12-well plate. The next day, C2C12 cells were switched from growth medium to differentiation medium [DMEM containing 2% horse serum and insulin (100ng/ml)] at confluence to induce differentiation. For the transient transfection, C2C12 cells were transfected with pCAGGS or pCAGGS-MV-N using the 4D-Nucleofector system (Lonza; program CM-137 and SF cell line 4D-Nucleofector X kit) following the manufacturer`s instructions. After overnight incubation, the transfected cells were seeded in a 12-well plate and induced to differentiate. For the infection of MV, C2C12 cells were seeded in a 12-well plate and infected with MV-EGFP (Terao-Muto et al. 2008) at a multiplicity of infection (MOI) of 1 (as determined on B95a cells). The next day, the infected cells were induced to differentiate. The protease inhibitors E64d and pepstatin A were purchased from the Peptide Institute (Osaka, Japan), and added to cells at 10μg/ml 24h before harvest to inhibit lysosomal degradation of autophagosomes.

.

Immunofluorescence staining of C2C12 cells

Cells were fixed with 2% paraformaldehyde at room temperature for 10min and permeabilized with PBS plus 0.2% Triton X-100 at room temperature for 10min. Blocking was performed with Blockace as described above. After that, cells were incubated with anti-myosin (My-32, Sigma), anti-p62 (2c11) mouse mAb (Abnova) and anti-MV-N rabbit polyclonal antibody for 1 hour at room temperature or overnight at 4°C. Secondary antibodies used were conjugated with Alexa 405, Alexa 488 or Alexa 568 (Invitrogen). DNA was counterstained with Hoechst 33342 (Lonza). Cells were observed by confocal fluorescence microscopy.

Western blot analysis of C2C12 cells

C2C12 cells were lysed with Laemmli`s buffer and boiled for 5 min at 100°C. Samples were subjected to SDS-10% or 15% polyacrylamide gel electrophoresis and transferred to polyvinylidene difluoride (PVDF) membrane. The membranes were blocked with Blockace as described above and then exposed to primary antibody (1:1000 dilution) for 1 hour at room temperature or overnight at 4°C, followed by incubation with a horseradish peroxidase-conjugated secondary antibody (Dako) for 1 hour at room temperature. Signals were detected by ECL Prime Western blotting detection reagent (GE Healthcare) using LAS-4000 image analyzer (Fujifilm). The following antibodies were used as primary antibodies: anti-MV-N rabbit polyclonal antibody, anti-LC3A/B rabbit polyclonal antibody (Cell signaling), anti-p62 (2c11) mouse mAb (Abnova), anti-myosin (My-32) mouse mAb (Sigma), anti-GAPDH (6C5) mouse mAb (Chemicon).

RT-PCR analysis

Total RNA was extracted from C2C12 cells using ISOGEN(Nippon Gene). The extracted RNA was treated with DNase I (Roche), and reverse-transcribed using PrimeScript® Reverse Transcriptase (Takara Bio Inc.) by random hexamer priming or oligo dT priming. The resultant cDNA was PCR-amplified using Phusion high-fidelity DNA polymerase (Finnzymes). For detection of the p62 mRNA, The following primers were used: forward primer, 5`-CAGCTGTTTCGTCCGTACCT-3`, and reverse primer, 5`-AAAAGGCAACCAAGTCCCCA-3`. The GAPDH-specific primers described in Chapter 1 were used as internal control.

RESULTS

The myopathy in MV-N mice resembles h-IBM.

Skeletal muscle taken from #36 described in Chapter 1 showed a irregular fiber size, rimmed vacuoles, and centralized nuclei consistent with h-IBM (Broccolini et al. 2009) (Figure 2-1). The rimmed vacuoles were also observed in cardiac muscle of MV-N mice. Therefore, the author focused on the similarity between myopathology of symptomatic MV-N mice and hereditary inclusion body myopathy (h-IBM). There are several reports that describe a detection of accumulation of phosphorylated tau (p-tau) and ubiquitinated proteins in cytoplasmic inclusion bodies of h-IBM patients (Broccolini et al. 2009). In cases of measles, tau- and ubiquitin-positive neurofibrillary tangles are demonstrated in subacute sclerosing panencephalitis (SSPE) patient (McQuaid et al. 1994). Based on these reports, the author hypothesized that the MV-N expressed in muscular system promoted accumulation of ubiquitin and p-tau. When the author immunostained with anti-ubiquitin antibodies, ubiquitin was detected as aggregates in cytoplasm of the skeletal muscle and cardiac muscle of symptomatic MV-N mice where MV-N formed inclusion-like structures (Figure 2-2). The ubiquitin aggregates were also strongly positive in enlarged nuclei of cardiac muscle of MV-N mice. In muscle tissues of WT mice, ubiquitin existed normally in nuclei. No ubiquitin immunoreactivity was seen in the smooth muscle of WT and symptomatic MV-N mice (data not shown). The distribution of tau protein in cardiac and skeletal muscle was the same, both in MV-N and WT mice, in contrast to our expectation. (Figure 2-3)

The accumulation of autophagy-related protein in the myopathic muscle of MV-N

The involvement of impaired autophagy system in myofiber degeneration has been suggested by detection of ubiquitin- and p62-positive protein aggregates in rimmed vacuolar myopathies

including h-IBM (Nishino 2003, Sandri 2010b). The author compared the distribution of autophagosome-associated proteins (p62/SQSTM1 and LC3) in ubiqutin-accumulated lesions with that in normal tissues. In ubiquitin-positive cardiac and skeletal muscle, p62-positive aggregates and vacuoles were also detected (Figure 2-2). These results indicate that the expression of MV-N in cardiac and skeletal muscle may induce the formation of inclusion bodies composed of ubiquitin, and p62 similarly to rimmed vacuolar myopathies (Sandri 2010b). In WT mice, The LC3 was not accumulated in both cardiac and skeletal muscle. However, in the skeletal muscle of symptomatic MV-N mice, LC3 was accumulated in the form of aggregates that were various-sized and often localized at the vacuole boundaries (Figure 2-2). The accumulation of LC3 in skeletal muscle suggested that the impairment of autophagy is related to formation of MV-N-induced inclusion body and degeneration of muscle. But the detailed mechanism is seemed to be different between cardiac and skeletal muscle.

MV-N inhibits myogenic differentiation in C2C12 myoblasts.

To further investigate the relevance of MV-N to myopathy, the author introduced MV-N into C2C12 mouse myoblasts. When myogenic differentiation is induced to C2C12, C2C12 cells start to fuse each other and transform into myotube (Figure 2-4A). After myogenic differentiation was induced, the level of myosin heavy chain (MyHC), a muscle differentiation marker, was low in MV-N expressing C2C12 cells relative to the corresponding of control cells (Figure 2-4B). This result indicates that MV-N inhibits muscle differentiation. The author wondered whether MV infection of C2C12 mouse myoblasts might inhibit myogenic differentiation because the MV infectivity to skeletal muscle was expected to be much lower than that to SLAM-expressing immune cells (Hashimoto et al. 2002). MV-infected mouse cell lines do not exhibit cytopathic effect (CPE) and the level of synthesized viral proteins is much lower than those in lytically infected cells (Yanagi et al. 1994).

Nevertheless, the myogenic differentiation of C2C12 cells was inhibited by MV-infection at a multiplicity of infection (MOI) of 1 (Figure 2-5). The inhibition effect on myogenic differentiation by MV was more strongly observed in cells infected with MV before induction of differentiation then those infected with MV after that (Figure 2-5). This result suggests that natural infection of MV can inhibit the myogenic differentiation in a skeletal muscle despite of its low infectivity.

Stably expressed MV-N increases autophagic flux and exhausts LC3 in C2C12 myoblasts.

It was reported that the formation and lysosomal turnover of autophagosome increased during myogenic differentiation of C2C12 cells (Tanida et al. 2006). The author investigated whether the autophagosome formation was altered differentiating C2C12 cells. Interestingly, the level of total LC3 and p62 was decreased in MV-N high-expressing C2C12 cells, only when induced to differentiate (Figure 2-6A). When autophagy is induced, LC3-I is lipidated to form LC3-II which attaches to autophagosomal membranes. The LC3-II is degraded by autolysosomes which are formed by fusion of autophagosomes and lysosomes (Mizushima, Yoshimori & Levine 2010). p62 is a famous autophagy substrate, which is not degraded by ubiquitin-proteasome system (Komatsu, Ichimura 2010). To eliminate the possibility that the p62 transcription is suppressed in MV-N expressing cells, the author confirmed that the level of p62 transcript was not changed in MV-N expressing cells (Figure 2-6D). Thus, the decreased level of LC3 and p62 suggested that the stably expressing MV-N increased the autophagy flux and exhausted the LC3.

The author tested whether lysosomal turnover of autophagosome occurred in MV-N expressing cell lines by using lysosomal inhibitors (E64d and pepstatin A). The amount of LC3-II was significantly increased by lysosomal inhibitors in control cells and MV-N low-expressing cells (N1), but not in MV-N high-expressing cells (N5 and N10), indicating the decreased lysosomal turnover of autophagosome in MV-N high-expressing cells (Figure 2-6B). The amount of LC3-II was not changed

by lysosomal inhibitors in all differentiation-induced cells (Figure 2-6C). This may be due to termination of autophagy required to differentiation.

The p62 aggregates were increased in differentiation-induced MV-N expressing C2C12 cells.

p62 forms aggregates with ubiquitinated proteins and is degraded by autophagy (Bjørkøy et al. 2005). The author wondered whether the p62 aggregates increased in MV-N expressing cells due to the LC3 exhaustion. The p62 distribution was basal level in both control and MV-N expressing cells before differentiation (Figure 2-7). Surprisingly, during myogenic differentiation, increased p62 aggregates were observed in MV-N expressing cell line except N10, in which p62 was significantly decreased (Figure 2-7). The increase of p62 aggregates also occurred in low-MV-N expressing cells (N1). These p62 aggregations in MV-N expressing cells imply the defect in protein degradation pathway in MV-N expressing cells.

DISCUSSION

In this chapter, the author characterized the myopathy observed in MV-N mice. The muscle degeneration seen in MV-N mice had similar characteristics to h-IBM. Ubiquitin and autophagy-associated proteins were accumulated in skeletal muscle (Figure 2-3). These results indicate that the accumulation of MV-N induced h-IBM-like phenotype through alteration of autophagy.

The myogenic differentiation was suppressed in MV-N expressing C2C12 cells (Figure 2-4). Furthermore, when myogenic differentiation was induced, the LC3 decreased in C2C12 cells strongly expressing MV-N. Because the p62 (autophagosomal substrate) level was also decreased in these cells, the decreased LC3 level is seemed to be outcome of LC3 overconsumption. Decrease of autophagosome results in accumulation of protein aggregates in atg-knock mice (Levine, Kroemer 2008). In MV-N expressing cells, p62 aggregates were increased during myogenic differentiation, whereas p62 expressed diffusely in control cells. The p62 aggregates may be degraded if the autophagy act normally; otherwise, the p62 aggregates may be detrimental to cells. These p62 aggregates in MV-N expressing cells were similar to the accumulation of ubiquitin and autophagy-related proteins in MV-N mice. The role of MV-N for autophagy requires further investigation on MV-N mice.

Autophagy degrades certain intracellular pathogens including viruses (Levine, Deretic 2007). Nevertheless, several studies have proposed that viruses may use autophagosomes as a scaffold of viral RNA replication complexes (Jackson et al. 2005). Viruses are seemed to have many ways to escape the degradation. Viral inhibition of autophagy was reported in HIV-1, influenza virus, and herpesviruses. In HIV-1 infection, the formation of autophagosome promoted HIV yields, but the degradation of HIV did not occurred due to the inhibition of autophagosome maturation by HIV protein Nef (Kyei et al. 2009). The maturation of autophagosome (the fusion of autophagosome with

the lysosome) was also blocked by matrix protein 2 (M2) of influenza A virus (Gannagé et al. 2009). Herpesviruses inhibit autophagy by binding with Atg3 and Beclin-1, and evade innate immunity and apoptosis (Lee et al. 2009, Orvedahl et al. 2007). The alteration of autophagic flux by MV-N might be one of the survival strategies of measles virus.

There are two possibilities for the contribution of MV-N to myopathy. First, myofibers may wane because of excessive autophagic flux induced by MV-N. Excessive autophagy participates in loss of muscle mass. LC3 and Gabarap genes are upregulated in atrophying muscle. (Zhao et al. 2007) In muscle atrophy models, the knockdown of LC3 palliated the muscle loss. (Dobrowolny et al. 2008, Mammucari et al. 2007) However, the muscle atrophy by MV-N is expected to be temporary because persistent expression of MV-N result in the exhaustion of LC3 which is essential for autophagosome formation. Second, abnormal accumulation of proteins may occur if the LC3 exhaustion also occurs in vivo. In MV-N mice, both the atrophy and protein accumulation were observed. This phenotype implies the MV-N induced both two phenotype by the respective mechanism. In the initial phase of MV-N expression, MV-N may induce atrophy of myofiber. However, if LC3 exhaustion occurs in myofibers like in the MV-N expressing cells, undegraded proteins should accumulate. The protein accumulation by MV-N may be weaker than that in lysosomal diseases because p62, which is needed to aggregate proteins (Komatsu et al. 2007), is also decreased in MV-N expressing cells. Nevertheless, p62 aggregates were observed in MV-N expressing cells. This means that the balance between the LC3 and p62 may determine the occurrance of protein aggregates in the MV-N expressing cell. Kurihara et al. showed the coexpression of MV-N and mutated p62 dramatically increased the Paget`s-like bone lesions in mice (Kurihara et al. 2011). The mutation of p62 used in this report induces larger p62 aggregates than wild type p62 (Leach et al. 2006). The increased p62 aggregates by the mutation may accelerate the outcome of LC3 exhaustion by MV-N.

In Chapter 2, MV-N showed altered autophagic flux in vivo and in vitro. Autophagy is involved in various biological processes such as starvation, cellular differentiation, cell death, aging, neurodegeneration, immunity, and cancer (Levine, Kroemer 2008, Mizushima, Levine 2010). The alterations in autophagy are involved in not only cardiac and muscle diseases but also neurodegenerative diseases, Crohn`s disease, and Paget`s disease (Mizushima et al. 2008), which are suspected to have relevance to MV (Honda et al. 2013, Wakefield et al. 1993, Kurihara et al. 2011). The results of Chapter 2 provide new insight into the role of MV-N in these autophagy-associated diseases.

FIGURE LEGENDS

Figure 2-1. Characteristics of myopathy seen in MV-N mice.

The morphology of transverse sections of cardiac and skeletal muscle was assessed by Hematoxylin staining. Rimmed vacuole (white arrows) and centralized nuclei (green arrows) are marked in skeletal muscle of MV-N mice with symptom. The rimmed vacuole was also observed in the cardiac muscle. The scale bar represents 50 μm.

Figure 2-2. Accumulation of ubiquitin, p62, and LC3 in cardiac and skeletal muscles of MV-N mice with symptom.

The paraffin-embedded tissues used in Figure 2-1 were cut into sections and immunostained with antibodies to ubiquitin, p62, and LC3. In WT mice, ubiquitin immunoreactivity was observed in the nuclei. In MV-N mice, ubiquitin expression in cytoplasm was enhanced relative to WT mice. Ubiquitin aggregates were observed in enlarged nuclei of cardiac muscle and cytoplasm. p62-positive aggregates and vacuoles were detected in MV-N mice. Accumulation of LC3 was observed in skeletal muscle of MV-N mice. The scale bar represents 50 μm.

Figure 2-3. Tau was not accumulated in MV-N mice with symptom.

The paraffin embedded tissues used in Figure 2-1 were cut into sections and immunostained with antibodies to tau. The distribution of tau was not altered in MV-N mice. The scale bar represents 50 μm.

Figure 2-4. MV-N inhibits myogenic differentiation in C2C12 cells.

(A) Illustration of the myogenic differentiation in C2C12 cells. C2C12 cells initiate to differentiate by

fusing each other when switching from growth medium to differentiation medium. The differentiated C2C12 cells express myosin heavy chain (MyHC). (B) C2C12 cells stably expressing MV-N (stable) or transiently transfected with MV-N (transient) were induced to differentiate. Immunofluorescence analysis was carried out 5 days (transient) or 7 days (stable) after induction of differentiation. Shown are the representative images stained for MyHC (green) and MV-N (red). Nuclei were counterstained with Hoechst 33342 (blue). The scale bar represents 100 μm. The number of MyHC-positive cells was decreased in MV-N expressing cells. The number of MyHC-positive cells was standardized with that in control culture. Each value represents the average ± standard deviation of triplicate cultures. (*P<0.05, Student`s t-test)

Figure 2-5. Myogenic differentiation was suppressed in MV-infected C2C12 cells.

C2C12 cells were infected with MV-EGFP (MV expressing the enhanced green fluorescent protein (Terao-Muto et al. 2008) 1 day before or 3 days after induction of differentiation (multiplicity of infection of 1) and subjected to immunofluorescence analysis at 7 days after induction of differentiation. The growth kinetics of MV-EGFP is comparable to that of wild-type MV. The number of MyHC-positive cells was decreased in MV-infected C2C12 cells. The number of MyHC-positive cells was standardized by the same method in Figure 2-4. Each value represents the average ± standard deviation of triplicate cultures. (*P<0.05, Student`s t-test) Representative images show the expression of MyHC (blue) and MV-N (red). The scale bar represents 100 μm.

Figure 2-6. MV-N inhibits autophagosome formation in differentiating C2C12 cells.

Lysates from stable C2C12 cell lines were prepared at the time point of 0 day or 7 days after differentiation induction, and analyzed by western blotting as described in the Methods. Lysosomal inhibitor (E64d and pepstatin A) were added at 10μg/ml 24h before harvest. (A) The level of total LC3

and p62 was decreased in MV-N high-expressing C2C12 cells (N5, N10) after the differentiation induction. (B) The alteration of autophagy-associated proteins in the presence of lysosomal inhibitors was compared in undifferentiated cells. The amount of LC3-II (an autophagosome marker) was significantly increased by lysosomal inhibitors in control cells and MV-N low-expressing cells (N1), but not in MV-N high-expressing cells (N5, N10). (C) The alteration of autophagy-associated proteins in the presence of lysosomal inhibitors was compared 7 days after differentiation induction. The amount of LC3-II was not changed by lysosomal inhibitors in all cells. (D) The p62 transcripts were analyzed by RT-PCR. No significant difference was observed between control cells and MV-N expressing cells. Mouse GAPDH transcripts were used as control.

Figure 2-7. The p62 aggregates were increased in differentiation-induced MV-N expressing C2C12 cells.

The distribution was same between control and MV-N expressing cell lines before myogenic differentiation. 7 days after differentiation, more amount of p62 aggregates were seen in MV-N expressing cell lines except C2C12-N10. The scale bar represents 100 μm.

Figure 2-1

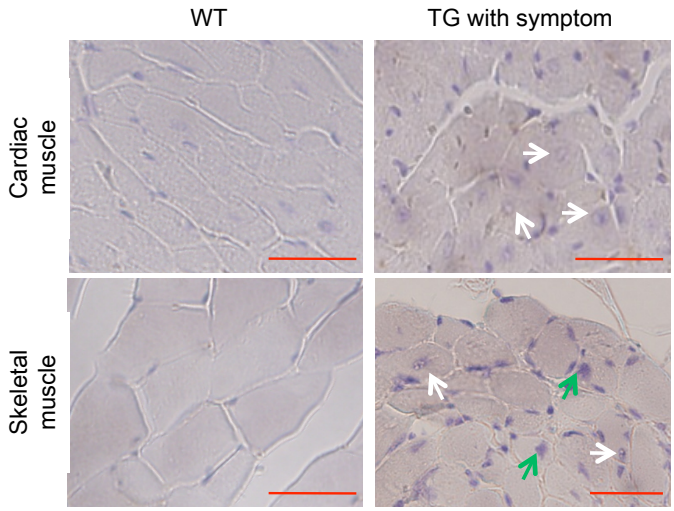

Figure 2-2

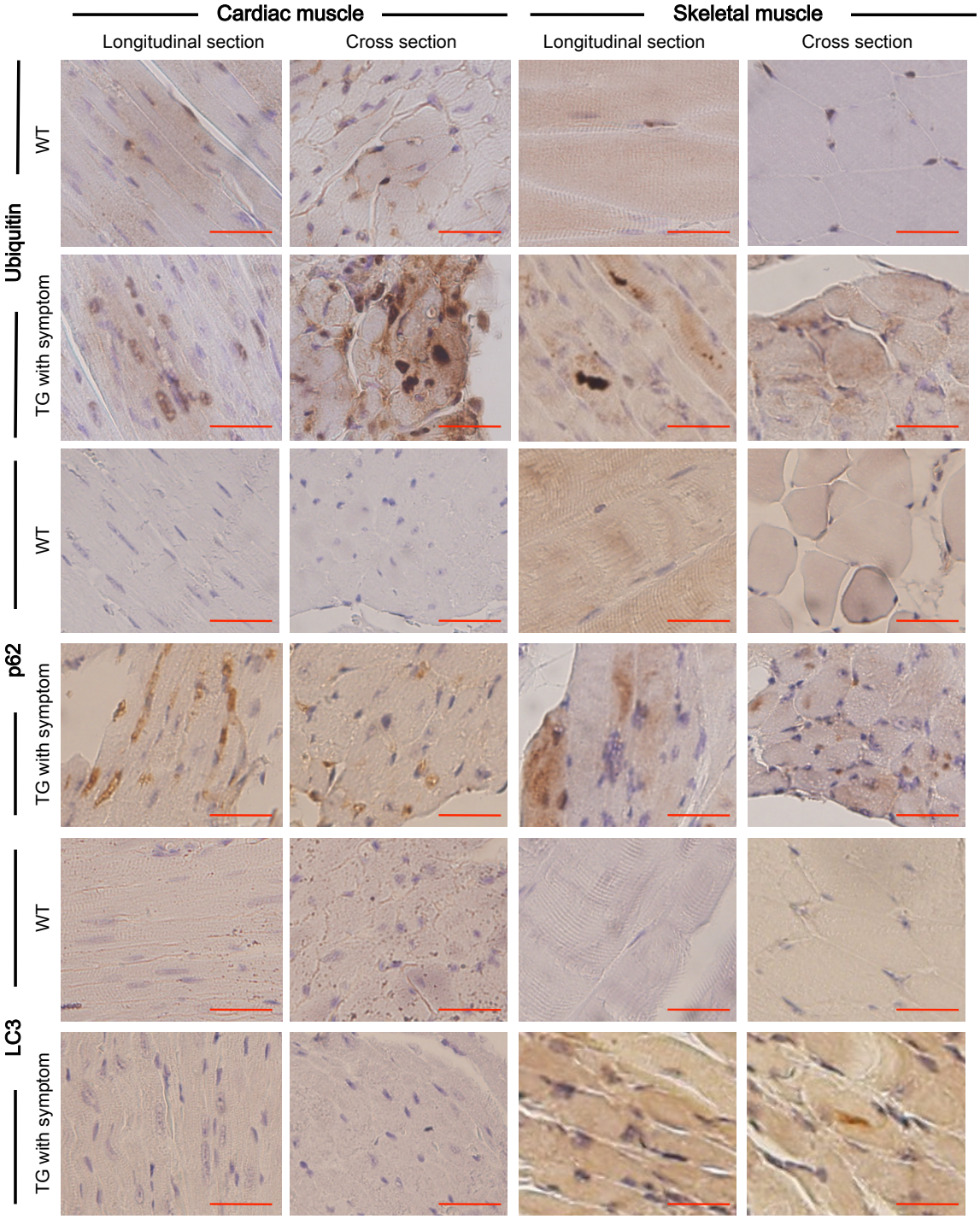
Cardiac muscle
Skeletal muscle
Longitudinal section
Cross section
Longitudinal section
Cross section
Ubiquitin
WT
TG with symptom
p62
WT
TG with symptom
LC3
WT
TG with symptom

Figure 2-3

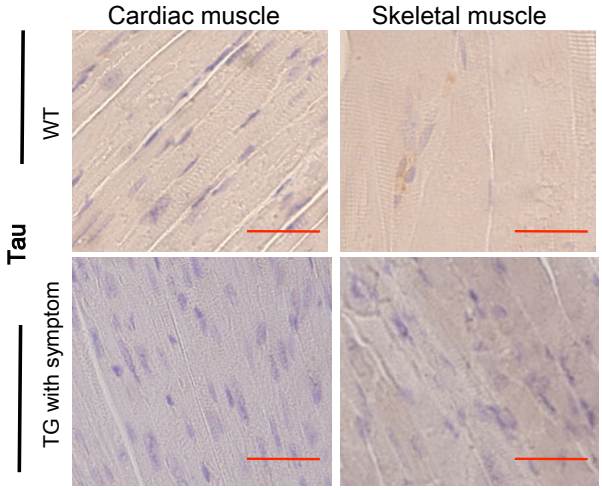

Figure 2-4

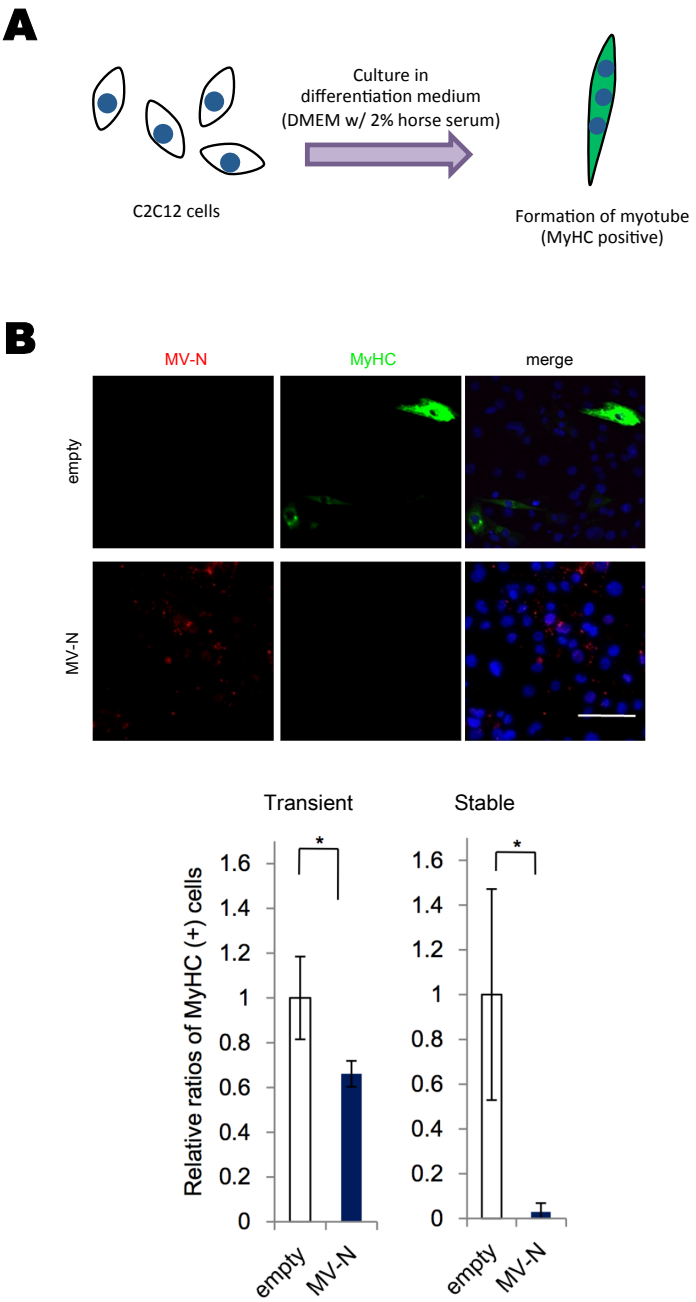
A
Culture in
differentiation medium
(DMEM w/ 2% horse serum)
C2C12 cells
Formation of myotube
(MyHC positive)
B
MV-N
MyHC
merge
empty
MV-N
Transient
Stable
Relative ratios of MyHC (+) cells
1.6
1.4
1.2
1
0.8
0.6
0.4
0.2
0
*
empty
MV-N

Figure 2-5

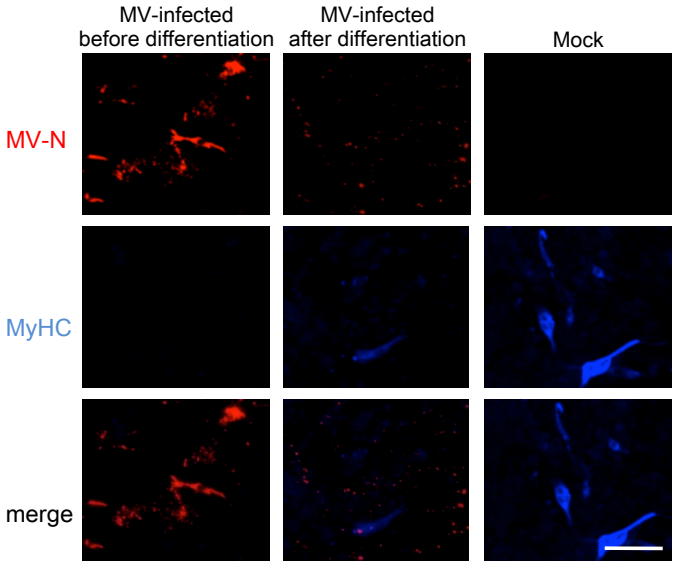
MV-infected
before differentiation
MV-infected
after differentiation
Mock
MV-N
MyHC
merge

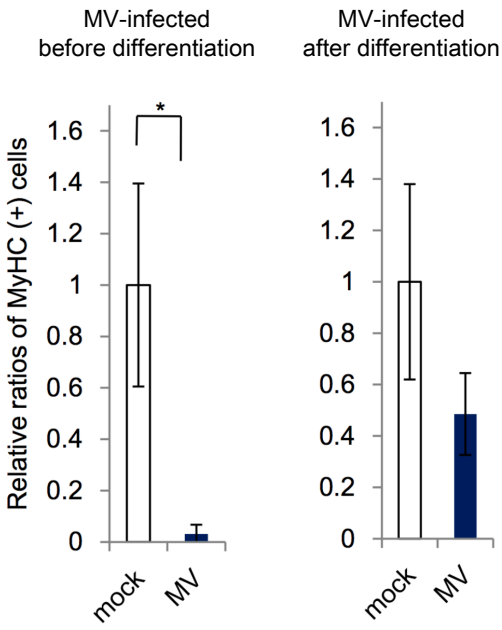
MV-infected
before differentiation
MV-infected
after differentiation
Relative ratios of MyHC (+) cells
1.6
1.4
1.2
1
0.8
0.6
0.4
0.2
0
*
mock
MV
mock
MV

Figure 2-6

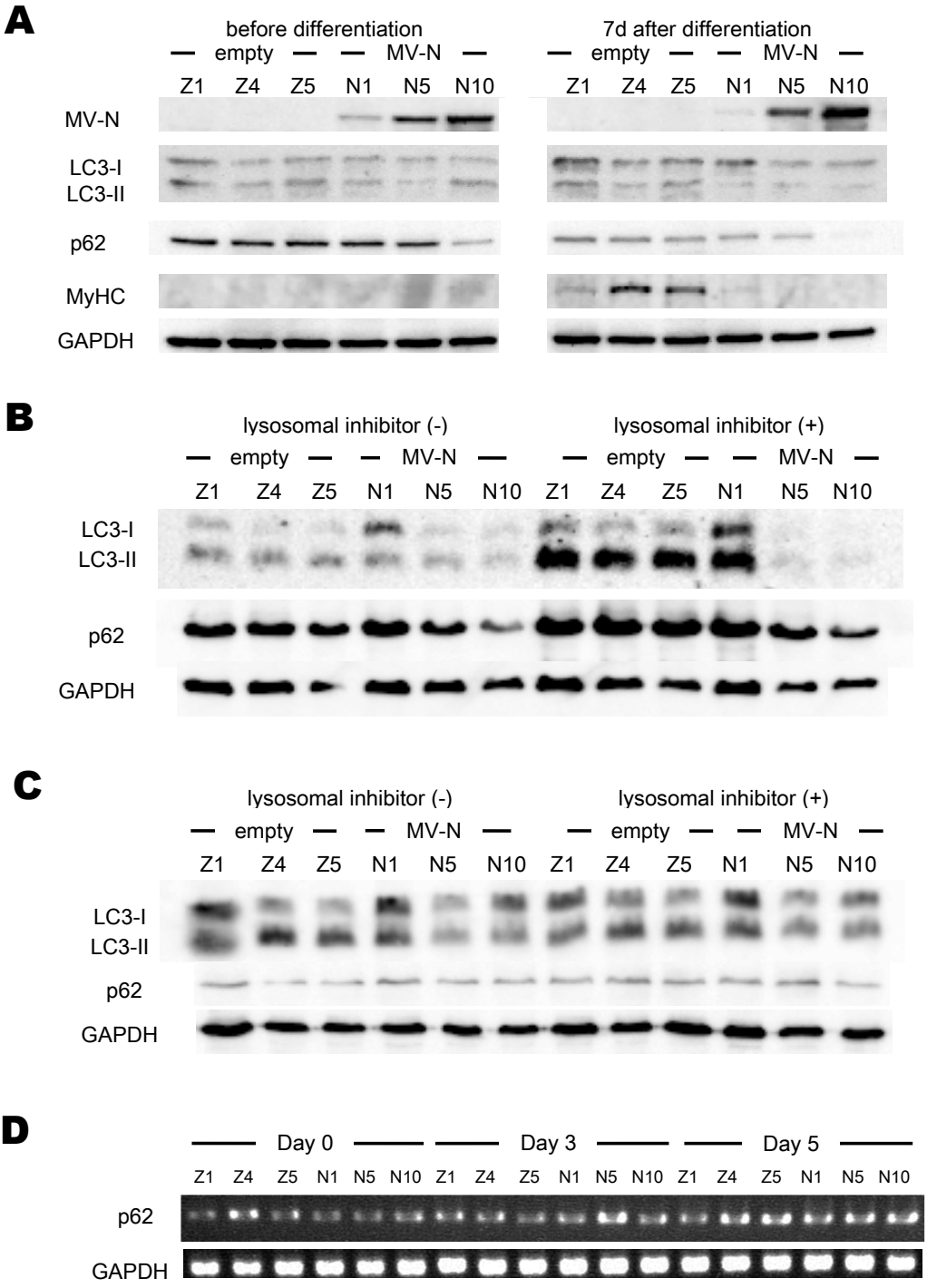
A
before differentiation
7d after differentiation
empty
MV-N
Z1 Z4 Z5 N1 N5 N10
MV-N
LC3-I
LC3-II
p62
MyHC
GAPDH
B
lysosomal inhibitor (-)
lysosomal inhibitor (+)
empty
MV-N
Z1 Z4 Z5 N1 N5 N10
LC3-I
LC3-II
p62
GAPDH
C
lysosomal inhibitor (-)
lysosomal inhibitor (+)
empty
MV-N
Z1 Z4 Z5 N1 N5 N10
LC3-I
LC3-II
p62
GAPDH
D
Day 0
Day 3
Day 5
Z1 Z4 Z5 N1 N5 N10 Z1 Z4 Z5 N1 N5 N10 Z1 Z4 Z5 N1 N5 N10
p62
GAPDH

Figure 2-7

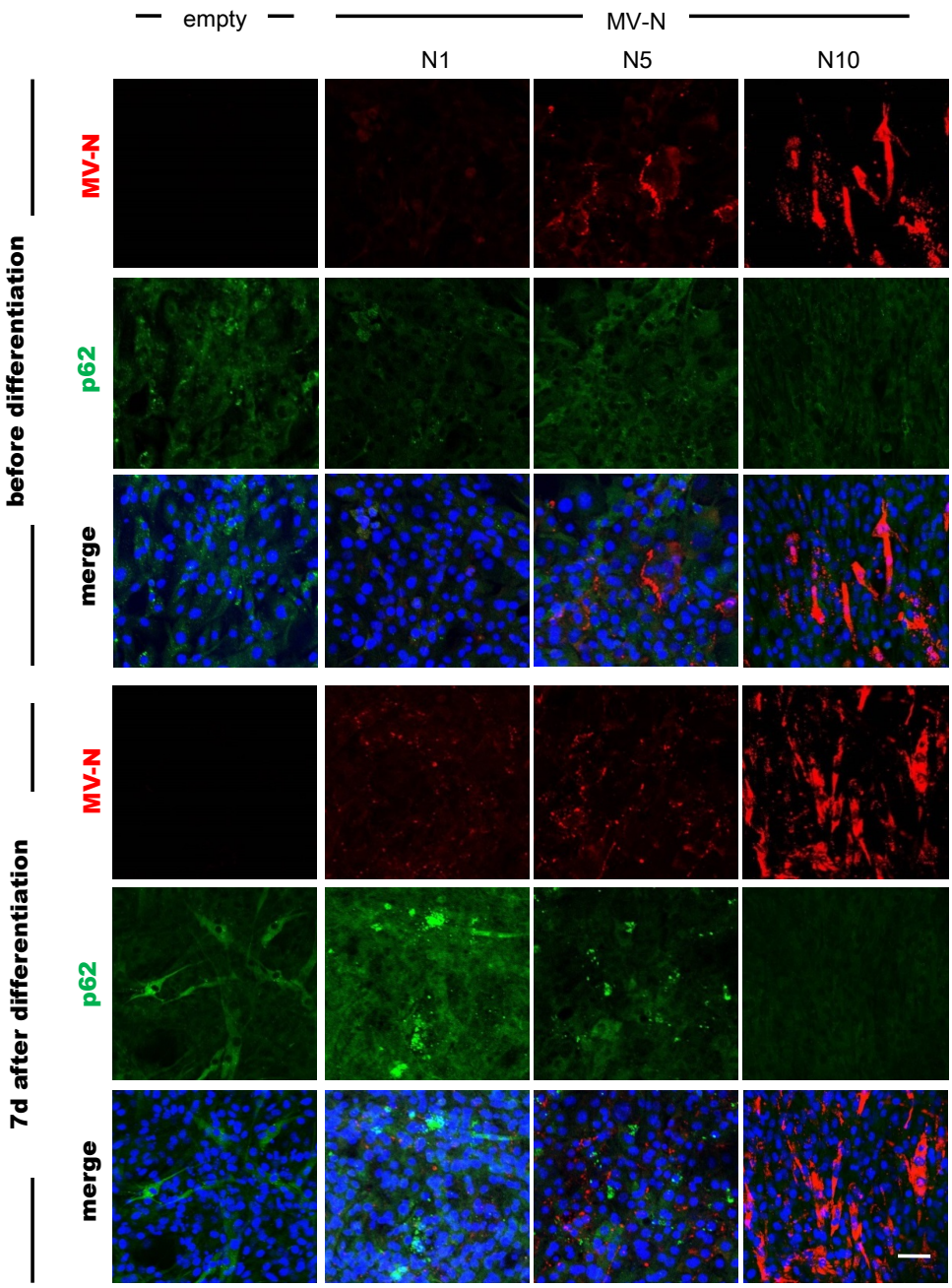
empty
MV-N
N1
N5
N10
before differentiation
7d after differentiation
MV-N
p62
merge
MV-N
p62
merge

CHAPTER 3

The effect of measles virus nucleocapsid protein on neuropathology

ABSTRACT

Measles virus (MV) causes subacute sclerosing panencephalitis (SSPE), a fatal disease of central nervous system occurred long after the acute infection. For the development of efficient diagnosis and treatment of SSPE, the elucidation of pathogenesis is needed. In Chapter 3, the author found that neurological symptoms occurred in some of MV-N mice. The MV-N expression in brain was increased in mice with symptoms, and the neuronal degeneration, loss of dendrites, and TDP-43 proteinopathy were observed in the MV-N expressing brain region. Furthermore, MV-N inhibited retinoic acid-induced neuronal differentiation and elevated the autophagic flux in mouse neuroblastoma N2a cells. This study suggests that the neurodegeneration is induced by MV-N expression. Thus, MV-N mice generated in this study are useful model to unravel the pathogenesis of SSPE and associated neurodegenerative diseases.

INTRODUCTION

Measles virus (MV) causes subacute sclerosing panencephalitis (SSPE), a persistant infection of MV, occurred long after the acute infection. SSPE strains have distinct characteristics from typical measles virus strains. SSPE strains have mutations in M protein and F protein frequently (Cattaneo et al. 1989). These mutations are inferred to contribute to the loss of virions (Rima, Paul Duprex 2005).

SSPE is a progressive fatal disease of the central nervous system. The clinical characteristics of SSPE are variable, such as behavioral changes, cognitive decline, myoclonic jerks, seizures and optic disturbances (Garg 2008, Brismar et al. 1996). In the early phase of SSPE, the lesions are primarily arisen in the occipital regions of brain and spread to anterior portion of the cortex (Mawrin et al. 2002). Histopathologically, inflammatory infiltration around brain vessels, white matter demyelination, neuronal loss, and astrogliosis are observed in SSPE patients (Garg 2008). The symptoms of SSPE are non-specific and confused with other neurological diseases. The diagnosis of SSPE is confirmed by raised antimeasles antibody titers of cerebrospinal fluid or detection of MV RNA genome from brain tissues. So far available treatment of SSPE is still not developed. Thus, The development of efficient diagnosis and treatment of the disease is necessary.

In ultrastructural study of SSPE patients, the MV inclusion bodies were found in neurons and oligodendrocytes (Lewandowska et al. 2001). However, It still remains unknown how these inclusion bodies impact on the disease. It has been suggested that apoptosis of brain cells may contribute to the neuropathogenesis of measles virus (McQuaid et al. 1997). The apoptosis was also observed in virus-negative cells in the brain of SSPE patients. Thus the apoptosis is considered to be an indirect effect of MV infection, such as cytokine-mediated responses.

The N protein is the main component of the MV inclusion body. In the brains of SSPE patients, the N proteins are accumulated in the nuclei of infected cells (Liebert et al. 1986). However,

in acute infection, most of N proteins are distributed in the cytoplasm because N proteins are retained in cytoplasm by P proteins (Huber et al. 1991, Rima, Paul Duprex 2005). Altered nuclear body differentiation was noted in virus-positive cells in study of canine distemper virus subacute encephalitis, which is similar to SSPE (Oglesbee 1992). These results suggest that the N protein may have pathological function in nucleus of persistently infected cell.

In Chapter 3, the author found that neurological symptoms occurred in some of MV-N mice. The MV-N expression of brain was increased in mice with symptoms, and the neuronal degeneration was observed in MV-N expressing region. Furthermore, MV-N inhibited the neurite outgrowth in mouse N2a neuroblastoma cells.

MATERIALS AND METHODS

Mice

Four F_0 MV-N mice were generated in Chapter 1. Two F_0 MV-N mice without wasting symptom were bred and maintained. The MV-N mice used here were the second-generation progeny of MV-N mice.

Histopathological examination

Tissues of mice were fixed in Mildform® (Wako Pure Chemical Industries), dehydrated, embedded in paraffin, sectioned at 5μm. Brain tissues were stained with Luxol fast blue/cresyl violet (LFB/CV) and examined by light microscopy.

Immunohistochemical analysis

For immunohistochemical analysis, following antibodies were used as primary antibodies: anti-MV-N rabbit polyclonal antibody, anti-GFAP rabbit polyclonal antibody (Sigma), anti-MAP2 mouse mAb (Chemicon), anti-TDP-43 rabbit polyclonal antibody (Proteintech), and anti-ubiquitin (P4D1) mouse mAb (Cell signaling). Paraffin sections were deparaffinized, rehydrated, and submitted to heat-mediated antigen retrieval. As an antigen retrieval buffer, author used EDTA buffer (1mM, pH 8.0) for MV-N and citrate buffer (10mM, pH 6.0) for GFAP, MAP2, TDP-43, and ubiquitin. Antigen-retrieved sections were processed to immunostaining as described in Chapter 1.

Cell culture and induction of neuronal differentiation

Mouse neuroblastoma N2a cells were grown in Dulbecco`s minimal essential medium (DMEM) containing 10% fetal calf serum (FCS). For the induction of neuronal differentiation, the

growth medium were switched to DMEM containing 2% FCS and 20μM retinoic acid. The medium was changed every 24h. Cells with a neurite longer than twice the diameter of the cell body were judged as differentiated (Cowley et al. 1994).

Transfection of N2a cells

For the transient transfection of N2a cells, 5×10^4 cells were plated in a 24-well plate. The next day, N2a cells were tranfected with pCAGGS or pCAGGS-MV-N using Lipofectamine LTX (Invitrogen) following the manufacturer`s instructions.

Immunofluorescence staining of N2a cells

Cells grown on coverslips in a 24-well plate were proceeded to fixation, permeabilization, and immunostaining as described in Chapter 2. As primary antibody, anti-canine distemper virus N protein mouse mAb 8G [an antibody cross-reacting with MV-N (Masuda et al. 2006)] and anti-beta-tubulin III rabbit polyclonal antibody (Abcam) were used.

Western blot analysis of N2a cells

The sample preparation, SDS-PAGE and western blots were performed as described in Chapter 2. The protease inhibitors E64d and pepstatin A (Peptide Institute) were added to cells at 10μg/ml 24h before harvest to inhibit lysosomal degradation of autophagosomes. The following antibodies were used as primary antibodies: anti-MV-N rabbit polyclonal antibody, anti-beta-tubulin III rabbit polyclonal antibody (Abcam), anti-TDP-43 rabbit polyclonal antibody (Proteintech), anti-p62 (2c11) mouse mAb (Abnova), anti-LC3A/B rabbit polyclonal antibody (Cell signaling), and anti-GAPDH (6C5) mouse mAb (Chemicon).

RESULTS

The neurological symptoms in MV-N transgenic mice.

Two out of the four F_0 MV-N mice produced in Chapter 1 were bred and maintained. As a result of breeding, 18 males and 31 females were maintained over one year. Of these mice, two male mice (#57 and #71) showed neurological symptoms at 16 and 20 months of age. Two mice showed circus movement when they were suspended by their tail. These two mice usually exhibited reduced activity. Mice having neurological symptoms were sacrificed and examined 1 week and 3 weeks after the onset of symptoms.

The MV-N mice with neurological symptoms showed different MV-N expression pattern from MV-N mice without symptom.

In order to assess the relevance between MV-N expression and neurological symptom, the author performed immunohistochemical analyses on brains of MV-N mice (Table 3-1). In MV-N mice with neurological symptoms, MV-N was detected in neurons of cerebral cortex, diencephalon, mesencephalon, and medulla of #57 and all region of #71 (Figure 3-1). In MV-N mice without neurological symptom, MV-N was detected in diencephalon and cerebellum region (Figure 3-2). In diencephalon region, the MV-N immunoreactivity was limited in hypothalamus. These results indicate that MV-N expression was increased in the cerebral cortex, diencephalon, mesencephalon, and medulla regions of MV-N mice with neurological symptoms relative to those without symptom.

The lesions of MV-N mice with neurological symptoms

The author examined the brain sections of the MV-N mice using luxol fast blue/cresyl violet (LFB/CV) stain. Loss of neuron in cerebral cortex was observed from MV-N mice with neurological

symptoms (Figure 3-3A). Degenerative neurons were also noted in these cerebral cortex lesions (Figure 3-3B). Demyelination in left cerebral peduncle was also observed in #57 (Figure 3-3A).

Some markers of brain cells were analyzed by immunohistochemistry. MAP2, a dendritic marker, was not detected in cerebral cortex lesion (Figure 3-4). There was no difference between normal tissues and lesions in GFAP (astrocytic marker) immunostaining (Data not shown). These results confirmed that degeneration of neurons was occurred in MV-N expressing cerebral cortex.

Development of TDP-43 proteinopathy in MV-N mice with neurological symptoms

The author detected TDP-43 proteinopathy in MV-N mice with neurological symptoms. Ubiquitinated TDP-43 is the major disease protein in the frontotemporal lobar degeneration (FTLD-U) and Amyotrophic lateral sclerosis (ALS) (Neumann et al. 2006). In normal brains, TDP-43 distributes in the nuclei of neurons. In the brains of FTLD-U patients, the expression of TDP-43 in nuclei was dramatically reduced, and cytoplasmic TDP-43 aggregates were detected (Kwong et al. 2007). Author investigated the distribution of TDP-43 in the brains of MV-N mice. The loss of nuclear TDP-43 staining was detected in one out of eight MV-N mice without neurological symptom (Data not shown) and all MV-N mice with neurological symptoms (Figure 3-5). In MV-N mice with neurological symptoms, the loss of nuclear TDP-43 staining was detected in where MV-N expression was detected, except hippocampus, medulla, cerebellum region of #71.

MV-N inhibits retinoic acid-induced differentiation of N2a cells.

The neuronal degeneration seen in MV-N mice suggest that MV-N may have some roles in degeneration of neuron. To examine the function of MV-N in neuron, the author transfected mouse neuroblastoma N2a cells with MV-N. The N2a cells were differentiated using retinoic acid (RA) treatment for four days (Shea, Fischer & Sapirstein 1985). In undifferentiated N2a cells, cellular

morphology and viability were not different between MV-N expressing cells and control ones (Figure 3-6A and data not shown). However, when neuronal differentiation was induced in N2a cells, the neurite outgrowth was suppressed in MV-N expressing N2a cells (Figure 3-6).

The neuronal differentiation was also assessed in MV-infected N2a cells. The MV infectivity to N2a cells was low and cytopathic effect (CPE) was not occurred in MV-infected N2a cells (Figure 3-7A). However, the neurite outgrowth of differentiation-induced cells was inhibited by MV infection (Figure 3-7).

Increase of the autophagic flux by MV-N in differentiation-induced N2a cells.

To evaluate the change in MV-N expressing N2a cells, the author analyzed the neuronal marker beta-tubulin III and autophagy protein LC3 (Figure 3-8A). After the induction of differentiation, both beta-tubulin III and LC3-II (an autophagosome marker) were markedly increased. The level of TDP-43 was decreased slightly, but no difference was observed between control and MV-N expressing cells. Before differentiation, the amount of beta-tubulin III and LC3-II was approximately equal between MV-N expressing and control N2a cells. However, after differentiation, MV-N expressing N2a cells exhibited higher beta-tubulin III expression and lower LC3-II expression than control cells.

Then the author examined the expression of LC3-II under the presence of lysosomal inhibitors to determine whether lysosomal turnover of autophagosome occurred in N2a cells (Figure 3-8B). In differentiating N2a cells, the lysosomal turnover of autophagosome dramatically increased by MV-N. This result indicates the function of MV-N to elevate the autophagic function.

It is reported that the autophagy is activated during neuronal differentiation, and that either inhibition or stimulation of autophagy abrogates the differentiation (Zeng, Zhou 2008). Thus, the inhibition of neurite growth by MV-N seemed to be caused by altered autophagy. However, the

expression of beta-tubulin III was increased in MV-N expressing N2a cells unexpectedly. It is unclear and remains to be investigated how increased beta-tubulin III affect MV-N expressing N2a cells.

DISCUSSION

In this study, the author has analyzed the correlation between the neurological symptoms and MV-N expression in MV-N mice. In mice with neurological symptoms, the MV-N expression of cerebral cortex, midbrain, and medulla was increased relative to those without symptom. The neuronal degeneration and abnormal TDP-43 staining were also observed in MV-N expressing brain regions. The present data suggests that MV-N included in MV inclusion body may affect nervous system pathologically in persistant infection.

The neurological symptoms seen in MV-N mice is seemed to be linked to lesions of cerebral cortex because the lesions are common in MV-N mice with symptoms. The MV-N was detected in hypothalamus of MV-N mice without symptom. Nevertheless, no lesion was detected in the thalamus. In histopathological examination of mice with symptoms, the main lesion was the neuronal loss and degeneration. Author also examined for the presence of inflammation, demyelination, and astrogliosis which were seen in SSPE cases (Garg 2008). However, these lesions were not detected or were restricted to a focal area. This difference suggests that many lesions seen in SSPE may be affected by MV infection indirectly, and that the neuronal degeneration may be directly associated with MV-N.

Author observed the loss of dendrites in the cerebral cortex lesion of MV-N mice. The cerebral cortex dendritic degeneration was also reported in SSPE cases (Paula-Barbosa et al. 1980). Similar to the result of this chapter, an ultrastuctural study described that this dendritic change is likely subsequent to virus accumulation in dendritoplasm (Budka, Lassmann & Popow-Kraupp 1982). Author also found TDP-43 proteinopathy in brains of MV-N mice. Altered distribution of TDP-43 is a hallmark of neurodegeneration seen in several neurological disorders, such as FTLD-U and ALS (Janssens, Van Broeckhoven 2013). TDP-43 is a highly conserved nuclear RNA-binding protein involved in transcription and splicing regulation (Buratti, Baralle 2012). Mutation were identified in

various genes from the patients with TDP-43 proteinopathy. A number of mutated genes seen in these patients are thought to be associated with RNA processing and protein degradation. Thus, TDP-43 proteinopathy is considered as the result of impairment of RNA processing. MV-N can self-assemble into nucleocapsid-like structure without other MV components (Fooks et al. 1993). It is unknown whether nucleocapsid-like structure of MV-N contains cellular RNAs, but it was reported in other paramyvirus that sole expression of N results in the assembly of nucleocapsid-like structure containing cellular RNAs (Bhella et al. 2002). If MV-N can associate with cellular RNAs, it is expected that alteration of RNA processing by MV-N may occur like TDP-43 proteinopathy.

MV-N inhibits retinoic acid-induced differentiation of N2a cells. This result suggests that MV-N plays a role in neurodegeneration. To elucidate the mechanism of inhibition of neurite outgrowth by MV-N, the author examined the autophagy proteins. The autophagic flux was increased in MV-N expressing N2a cells as well as Chapter 2. The neuronal differentiation depends on a very delicate balance of autophagic activity. Inhibition of autophagy resulted in the defect of neuroal differentiation. But addition of rapamycin (an autophagy inducer) impaired the differentiation (Zeng, Zhou 2008). Autophagy also plays a homeostatic role in differentiated neurons by removal of damaged proteins and organelles, and the loss of autophagy causes neurodegeneration in mouse model (Komatsu et al. 2006, Hara et al. 2006). The downregulation of autophagy is observed in TDP-43 proteinopathies, but the mechanism is still under investigation. Wang, et al have proposed two possibilities for this phenomenon (Wang, Tsai & Shen 2013). First, the cytosolic TDP-43 inclusions may trap the p62, essential for the autophagy. Second, the autophagy-related mRNA may become unstable due to the loss-of-function of TDP-43. Further investigation of autophagy and TDP-43 function in author`s in vivo and in vitro model should provide valuable insights to clarify the mechanism of neurodegeneration.

This study offered new prospects for revealing the mechanism of neurodegeneration by measles infection. The MV virions disappeared in SSPE lesions, but it was unknown which component of MV affected the lesion. Author observed the neurodegenerative lesions and inhibition of neuronal differentiation using only MV-N. Furthermore, the phenotypes seen in MV-N expressing cells showed the alteration of TDP-43 and autophagy. The studies of interaction of MV-N with TDP-43 and autophagy are expected to provide the available treatment of SSPE and associated neurodegenerative diseases.

FIGURE LEGENDS

Figure 3-1. MV-N expression in MV-N mice with a neurological symptoms

Tissues of MV-N mice with neurological symptom and wild-type mice at the same age were used in comparison. #57 showed a neurological symptom at 20 months of age. #71 showed the symptom at 16 month of age. MV-N immunostaining was performed on brain tissues of mice. In #57, MV-N expression was noted in the neurons of cerebral cortex, diencephalon, mesencephalon, and medulla. In #71, MV-N expression was observed in all region of brain. Illustration represents the expression pattern of MV-N. Areas that express MV-N were graded, with ++ being MV-N in both cells and matrix and + being MV-N in cells or matrix. The scale bar represents 50 μm.

Figure 3-2. MV-N expression in MV-N mice without neurological symptom

Tissues of MV-N mice without neurological symptom were immunostained with anti-MV-N at various ages: 2 mice at 2 months of age, 4 mice at 12 months of age, and 2 mice at 24 months of age. The relevance between the age and MV-N expression was not noted. MV-N was detected in diencephalon and cerebellum region. In diencephalon region, strong MV-N immunoreactivity was observed only in hypothalamus but not in other regions of diencephalon. Areas that express MV-N were graded with same method used in Figure 3-1. The scale bar represents 50 μm.

Figure 3-3. The lesions of MV-N mice with neurological symptoms

Luxol fast blue/cresyl violet (LFB/CV) stain was performed on brain sections of MV-N mice. (A) In #57, loss of neuron in cerebral cortex region (1) and demyelination in mesencephalon region (2) were noted. In #71, loss of neuron was noted in cerebral cortex (3) and diencephalon (4) regions. Right panels show an enlarged view of the boxed area in left panels. The scale bar represents 50 μm. (B)

Degenerative neurons were also detected in both #57 and #71. Panels show the enlarged views of both the normal region and lesion of MV-N mice.

Figure 3-4. Loss of dendrite in MV-N mice with neurological symptoms

Brain sections of MV-N mice were immunostained with anti-MAP2, a dendritic marker. MAP2 immunoactivity was reduced in cerebral cortex region in which loss of neuron confirmed by LFB/CV stain. The scale bar represents 50 μm.

Figure 3-5. Development of TDP-43 proteinopathy in MV-N mice with neurological symptoms

Brain sections of MV-N mice were immunostained with anti-TDP-43. Loss of normal nuclear TDP-43 staining patterns in neurons was detected in both #57 and #71. In MV-N mice without symptom, this alteration of TDP-43 staining was detected in 1 of 8 mice. Illustration represents the distribution of nuclear clearance of TDP-43. Areas where nuclear clearance of TDP-43 was seen were scored. Prominent nuclear clearance (>10% of counted cells) was scored as ++, and occasional nuclear clearance (<10% of counted cells) was scored as +. The scale bar represents 50 μm.

Figure 3-6. MV-N inhibits retinoic acid-induced differentiation of N2a cells.

N2a cells were treated with 20 μM retinoic acid (RA) for 4 days. MV-N was transfected into N2a cells a day before differentiation. (A) The neurite outgrowth was assessed by immunostaining of beta-tubulin III, a neuronal specific marker. In MV-N expressing N2a cells, neurite outgrowth was lesser than that of control cells. Representative images show the expression of MV-N (red) and beta-tubulin III (green). Nuclei were counterstained with Hoechst 33342 (blue). (B) Quantification of N2a cell differentiation. Each value represents the mean ± SD of triplicate cultures.

Figure 3-7. Retinoic acid-induced differentiation was suppressed in MV-infected N2a cells.

N2a cells were infected with MV-EGFP for 24 hours then treated with 20 μM retinoic acid (RA) for 4 days. (A) The neurite outgrowth was assessed by immunostaining of beta-tubulin III, a neuronal specific marker. In MV-infected N2a cells, neurite outgrowth was lesser than that of mock-infected cells. Representative images show the expression of MV-N (blue) and beta-tubulin III (red). (B) Quantification of N2a cell differentiation. Each value represents the mean ± SD of triplicate cultures.

Figure 3-8. Increase of the autophagic flux by MV-N in differentiation-induced N2a cells.

Lysates from N2a cells were prepared at the indicated time points in the absence (A) or presence (B) of lysosomal inhibitors (E64d and pepstatin A), and analyzed by western blotting as described in the Methods. (A) Beta-tubulin III and LC3-II were increased in differentiation-induced control cells. The level of TDP-43 and p62 was not changed significantly. In MV-N expressing cells, the amount of beta-tubulin III was increased but the amount of LC3-II was decreased relative to control cells. (B) In the presence of lysosomal inhibitors, the amount of LC3-II was more increased in MV-N expressing cells than that in control cells. The lysosomal turnover was evaluated by subtracting the level of LC3-II without lysosomal inhibitors from that with lysosomal inhibitors.

Table 3-1: Expression of MV-N in MV-N mice

	Cerebral cortex	Hippocampus	Diencephalon Mesencephalon	Medulla	Cerebellum
#57(20m)	+	-	+	++	-
#71(16m)	++	+	+	+	++
Mice without Neurological Symptom	-		++	-	+
	-		+	-	+
	-		++		
	-	-	++	-	
	-	-		-	-
	-			-	+
	-	+	+		
	-		++	+	

Figure 3-1

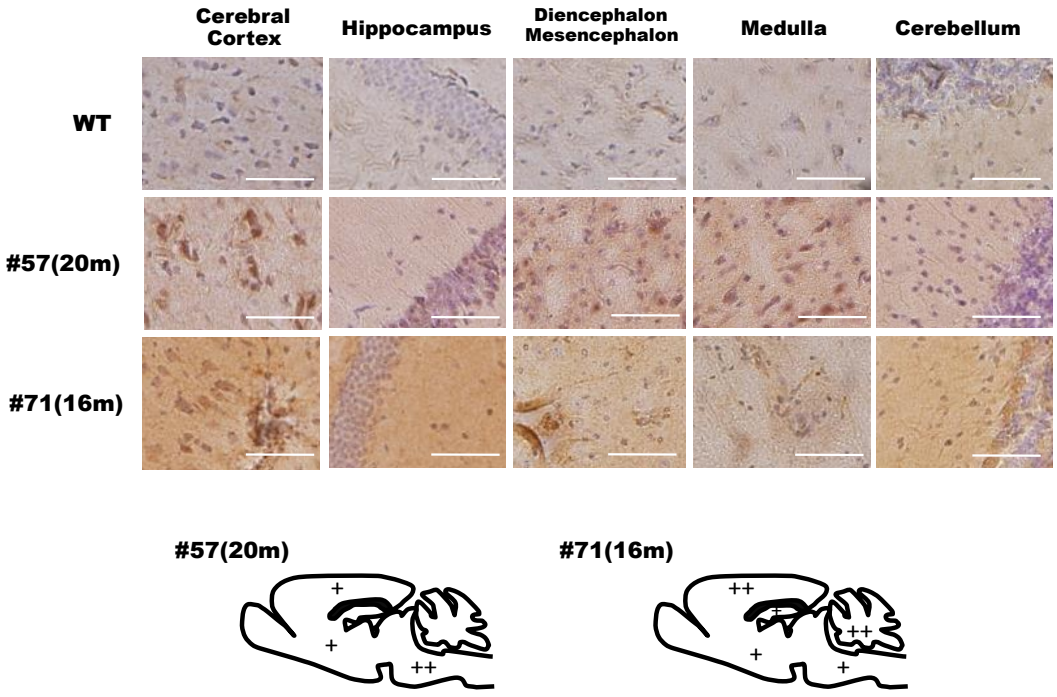
Cerebral Cortex
Hippocampus
Diencephalon Mesencephalon
Medulla
Cerebellum
WT
#57(20m)
#71(16m)
#57(20m)
+
+
++
#71(16m)
++
+
++
+
+

Figure 3-2

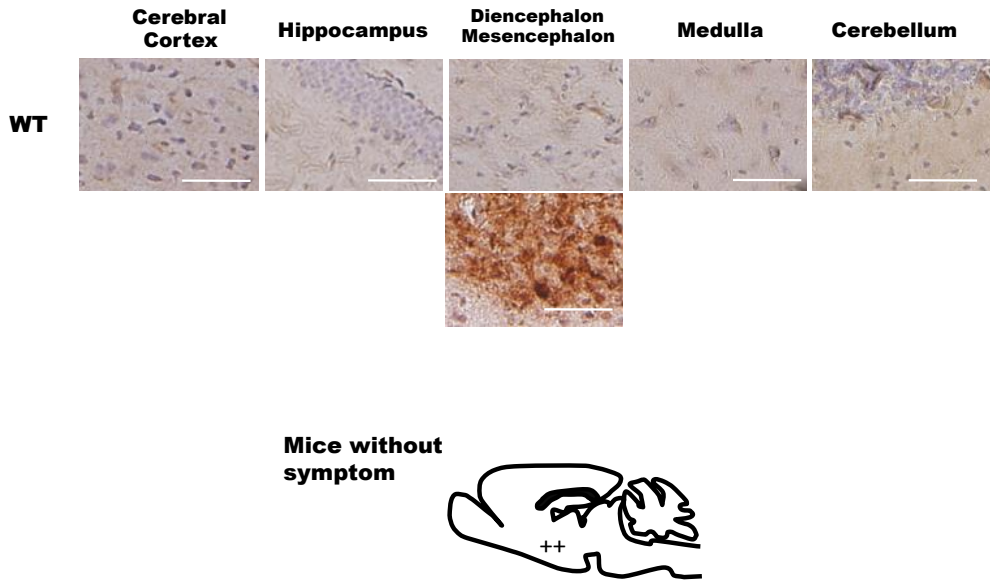
Cerebral Cortex
Hippocampus
Diencephalon Mesencephalon
Medulla
Cerebellum
WT
Mice without symptom
++

Figure 3-3

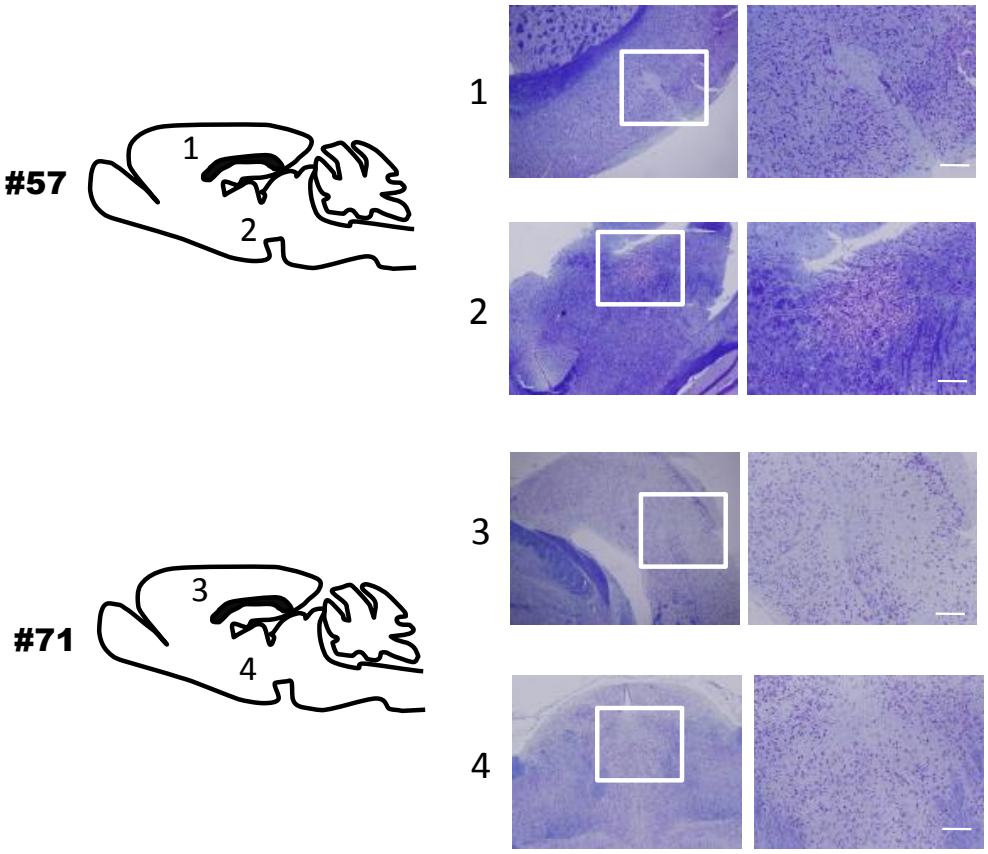

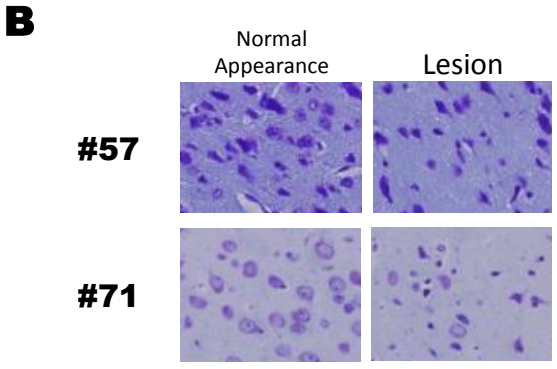

Figure 3-4

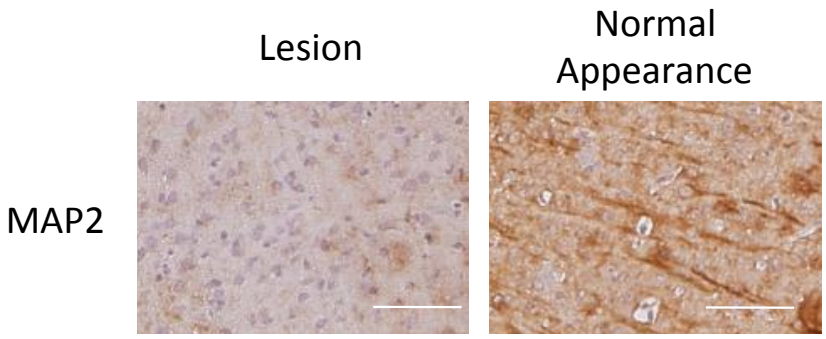

Figure 3-5

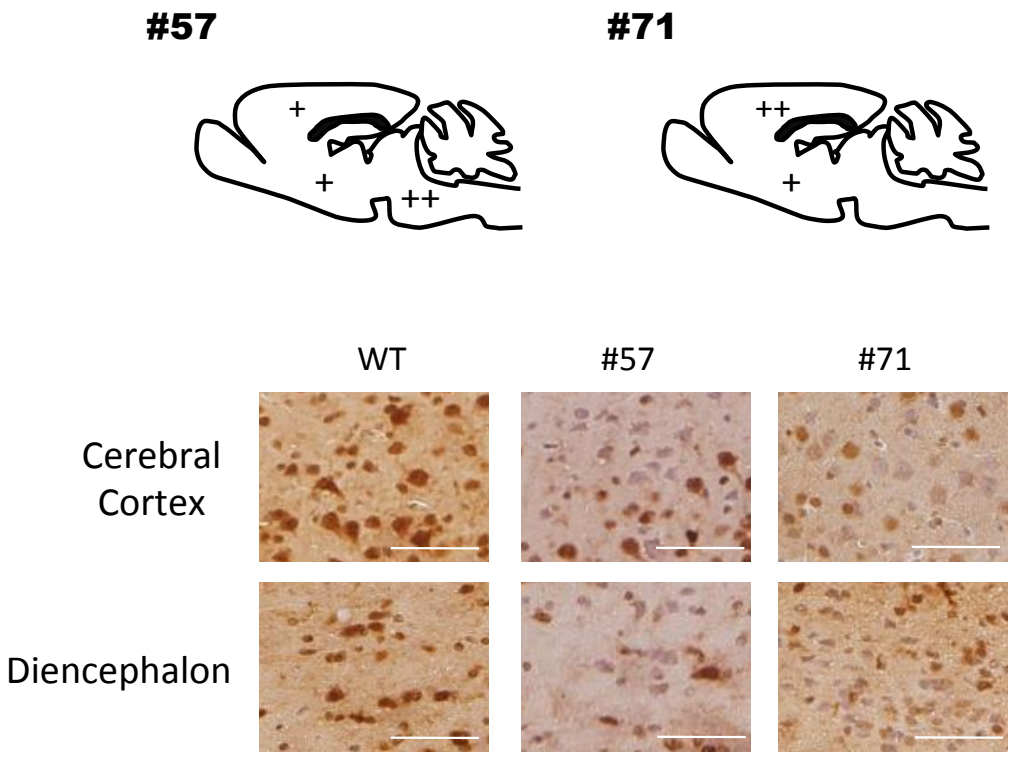

Figure 3-6

A

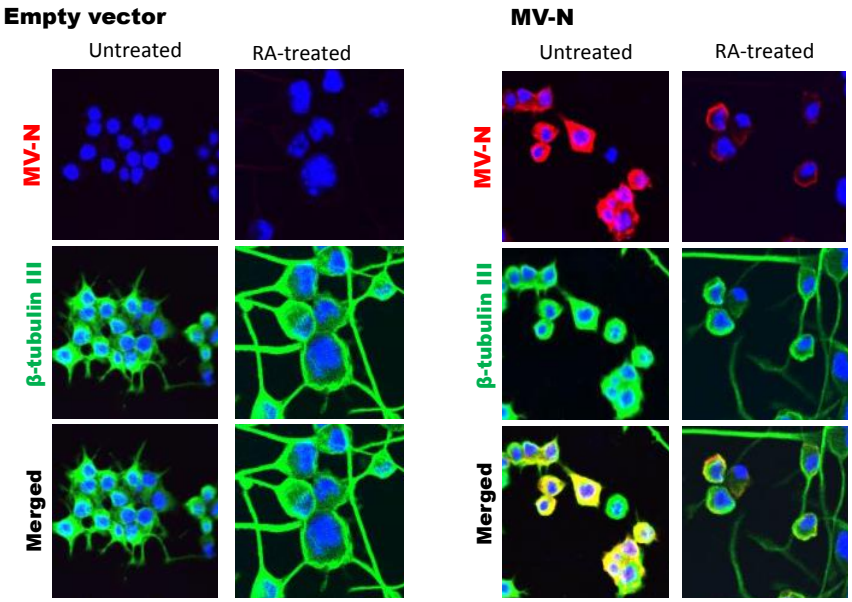
Empty vector
MV-N
Untreated
RA-treated
Untreated
RA-treated
MV-N
β-tubulin III
Merged
MV-N
β-tubulin III
Merged

B

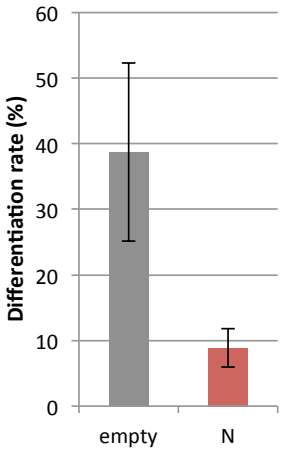
60
50
40
30
20
10
0
Differentiation rate (%)
empty
N

Figure 3-7

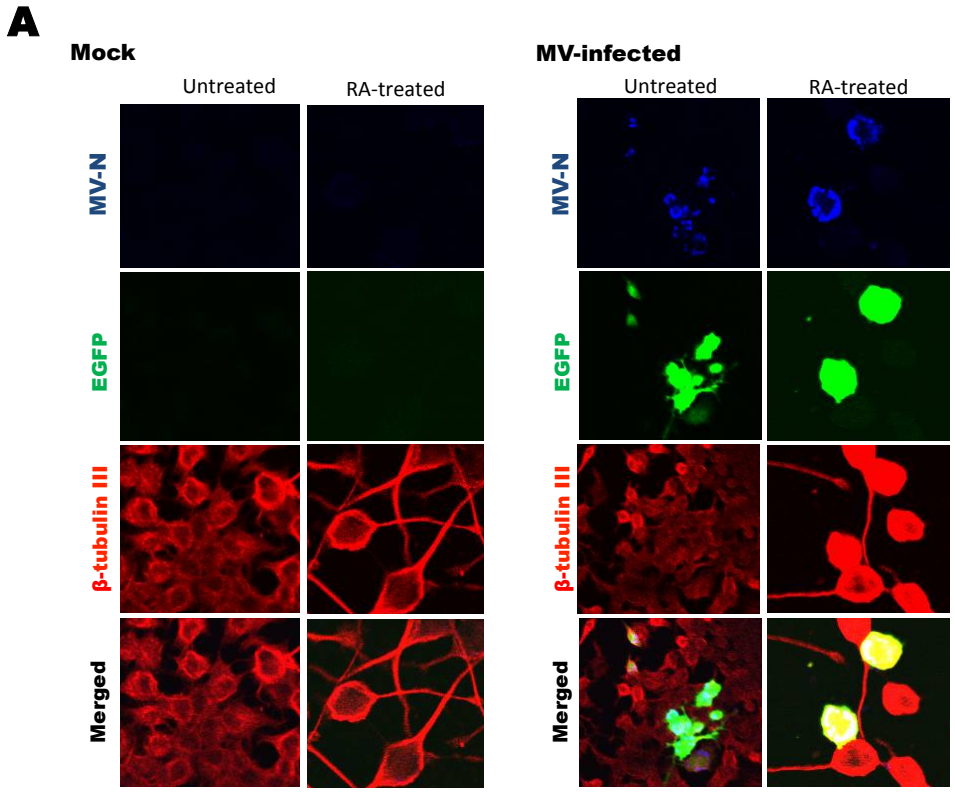
A
Mock
MV-infected
Untreated
RA-treated
Untreated
RA-treated
MV-N
EGFP
β-tubulin III
Merged
MV-N
EGFP
β-tubulin III
Merged

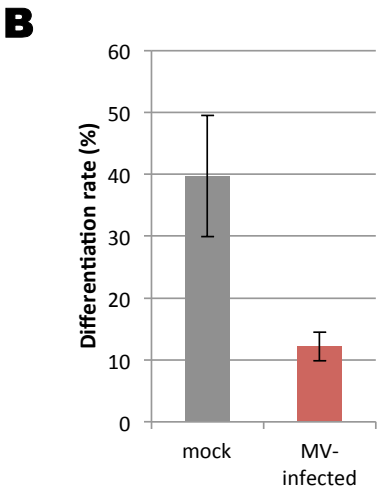
B
Differentiation rate (%)
60
50
40
30
20
10
0
mock
MV-infected

Figure 3-8

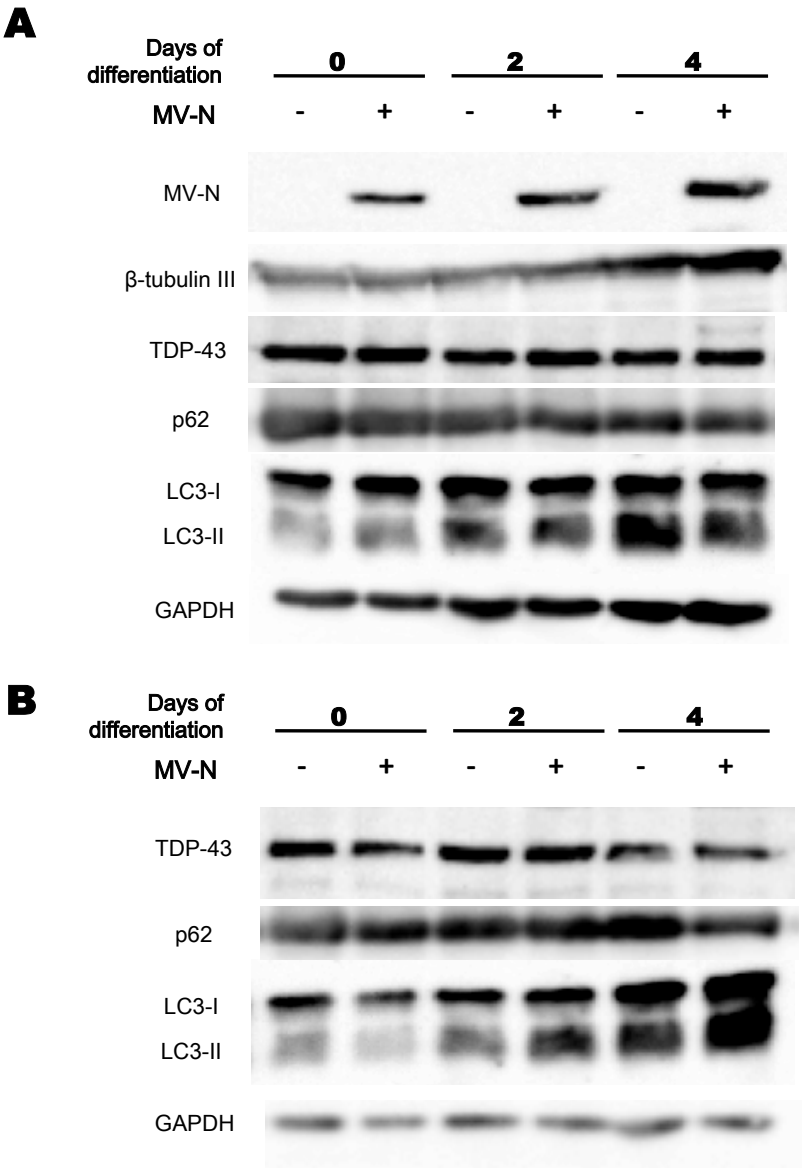
A
Days of differentiation
0
2
4
MV-N
- + - + - +
MV-N
β-tubulin III
TDP-43
p62
LC3-I
LC3-II
GAPDH
B
Days of differentiation
0
2
4
MV-N
- + - + - +
TDP-43
p62
LC3-I
LC3-II
GAPDH

CONCLUSION

Measles virus (MV), a member of the Morbillivirus genus in the Paramyxoviridae family, forms inclusion bodies in infected tissues regardless of the presence of infectious virion. MV inclusion bodies were assumed to participate in the pathogenicity of SSPE because the amount of the .inclusion bodies was proportional to the disease progression. Nevertheless, the function of MV inclusion bodies is still unclear. The author attempted to address the function of MV inclusion bodies by introducing MV-N, the main component of MV inclusion body, to mice and cells.

In Chapter 1, the author generated transgenic mice expressing MV-N. The expression of MV-N was restricted to the muscle tissues of a part of transgenic mice. The mice which expressed MV-N in their muscle tissues showed the wasting symptom and muscle degeneration. This phenotype strongly implied the effect of MV-N on myopathy.

In Chapter 2, the author focused on the features of myopathy that occurred in MV-N mice. The morphological features of myopathy in MV-N mice were similar to rimmed vacuolar myopathies, such as hereditary inclusion body myopathy (h-IBM). The author also found the accumulation of ubiquitin and autophagy-asssociated proteins in the degenerated muscles. In order to examine the association of MV-N with myopathy in detail, MV-N was introduced to the C2C12, a mouse myoblast cell line. The myogenic differentiation of C2C12 cells was inhibited by MV-N. The LC3, which is essential for the autophagosome formation, dramatically decreased in cells expressing MV-N strongly. The p62, which links ubiquitinated proteins to the autophagosome, was accumulated in MV-N after the induction of myogenic differentiation. These results indicate that MV-N may be implicated in myopathy by the alteration of autophagic flux.

In Chapter 3, author examined the association of MV-N with neurological symptoms occurred in old MV-N mice. The MV-N expression was increased in mice with neurological symptoms. The following characteristics were observed in the brain lesions of MV-N mice with symptoms: neuronal degeneration, loss of dendrites, and TDP-43 proteinopathy. In vitro, the author also found the inhibition of retinoic acid-induced neuronal differentiation and increase of autophagic flux in MV-N expressing mouse neuroblastoma N2a cells. These results suggest the neurodegeneration induced by MV-N.

The author generated MV-N mice for the examination of MV inclusion bodies in persistent infection, which mainly affect the nervous system. Unexpectedly, the phenotype of MV-N mice primarily appeared in muscles. This unexpected result provides a potential role of MV persistent infection on myopathy. Furthermore, the author observed the inhibition of myogenic differentiation and altered autophagic flux by MV-N in the mouse myoblast cell line. The effect of MV-N is also suggested in central nervous system by increased MV-N expression in mice with neurological symptoms and by inhibition of neurite outgrowth by MV-N. The findings from MV-N mice and MV-N expressing cells highlight the pathological function of MV-N in persistent infection of muscle and nervous system, and the alteration of autophagy flux by MV-N.

ACKNOWLEDGEMENT

I would like to express my gratitude to everyone who has contributed to this thesis, in particular to:

Professor Chieko Kai (Laboratory Animal Research Center, Institute of Medical Science, The University of Tokyo, Tokyo) for the invaluable support, critical encouragement and excellent scientific advice.

Research Associate Tomoyuki Honda (Laboratory of Human Tumor Viruses, Institute for Virus Research, Kyoto University, Kyoto), for the excellent scientific advice and great support.

Associate Professor Misako Yoneda (Laboratory Animal Research Center, Institute of Medical Science, The University of Tokyo, Tokyo), for the excellent scientific and technical advice.

Associate Professor Susumu Nakae and Dr. Aya Nambu (Laboratory of Sysytems Biology, Institute of Medical Science, The University of Tokyo, Tokyo), for the excellent technical advice and support.

Research Associate Hiroki Sato (Laboratory Animal Research Center, Institute of Medical Science, The University of Tokyo, Tokyo), for the excellent scientific and technical advice.

The colleagues of all members of Laboratory Animal Research Center, Institute of Medical Science, The University of Tokyo, for the encouragement and advice.

All animals for my studies for their lives.

My friends and family, for their kindness and continuous supports.

The Japanese Government Scholarship Program for giving me a chance to study in Japan.

These studies were supported by Grant-in Aid from the Ministry of Education, Culture, Sports, Science and Technology in Japan.

REFERENCES

Allen, I.V., McQuaid, S., McMahon, J., Kirk, J. & McConnell, R. 1996, "The significance of measles virus antigen and genome distribution in the CNS in SSPE for mechanisms of viral spread and demyelination", *Journal of Neuropathology & Experimental Neurology,* vol. 55, no. 4, pp. 471-480.

Axthelm, M. & Krakowka, S. 1998, "Experimental old dog encephalitis (ODE) in a gnotobiotic dog", *Veterinary Pathology Online,* vol. 35, no. 6, pp. 527-534.

Barth, P., Scholte, H., Berden, J., Van der Klei-Van Moorsel, JM, Luyt-Houwen, I., Van'T Veer-Korthof, E.T., Van der Harten, J. & Sobotka-Plojhar, M. 1983, "An X-linked mitochondrial disease affecting cardiac muscle, skeletal muscle and neutrophil leucocytes", *Journal of the neurological sciences,* vol. 62, no. 1, pp. 327-355.

Bellini, W.J., Rota, J.S., Lowe, L.E., Katz, R.S., Dyken, P.R., Zaki, S.R., Shieh, W. & Rota, P.A. 2005, "Subacute sclerosing panencephalitis: more cases of this fatal disease are prevented by measles immunization than was previously recognized", *Journal of Infectious Diseases,* vol. 192, no. 10, pp. 1686-1693.

Bellini, W., Englund, G., Rozenblatt, S., Arnheiter, H. & Richardson, C. 1985, "Measles virus P gene codes for two proteins.", *Journal of virology,* vol. 53, no. 3, pp. 908-919.

Bhella, D., Ralph, A., Murphy, L.B. & Yeo, R.P. 2002, "Significant differences in nucleocapsid morphology within the Paramyxoviridae", *Journal of general virology,* vol. 83, no. 8, pp. 1831-1839.

Bjørkøy, G., Lamark, T., Brech, A., Outzen, H., Perander, M., Øvervatn, A., Stenmark, H. & Johansen, T. 2005, "p62/SQSTM1 forms protein aggregates degraded by autophagy and has a protective effect on huntingtin-induced cell death", *The Journal of cell biology,* vol. 171, no. 4, pp. 603-614.

Bolt, G., Jensen, T.D., Gottschalck, E., Arctander, P., Appel, M., Buckland, R. & Blixenkrone-M, M. 1997, "Genetic diversity of the attachment (H) protein gene of current field isolates of canine distemper virus.", *Journal of General Virology,* vol. 78, no. 2, pp. 367-372.

Brismar, J., Gascon, G.G., von Steyern, K.V. & Bohlega, S. 1996, "Subacute sclerosing panencephalitis: evaluation with CT and MR.", *American Journal of Neuroradiology,* vol. 17, no. 4, pp. 761-772.

Broccolini, A., Gidaro, T., Morosetti, R. & Mirabella, M. 2009, "Hereditary inclusion‐body myopathy: Clues on pathogenesis and possible therapy", *Muscle & nerve,* vol. 40, no. 3, pp. 340-349.

Budka, H., Lassmann, H. & Popow-Kraupp, T. 1982, "Measles virus antigen in panencephalitis", *Acta Neuropathologica,* vol. 56, no. 1, pp. 52-62.

Buratti, E. & Baralle, F.E. 2012, "TDP-43: gumming up neurons through protein–protein and protein–RNA interactions", *Trends in biochemical sciences,* vol. 37, no. 6, pp. 237-247.

Campbell, H., Andrews, N., Brown, K. & Miller, E. 2007, "Review of the effect of measles vaccination on the epidemiology of SSPE", *International journal of epidemiology,* vol. 36, no. 6, pp. 1334-1348.

Carsillo, T., Carsillo, M., Traylor, Z., Rajala-Schultz, P., Popovich, P., Niewiesk, S. & Oglesbee, M. 2009, "Major histocompatibility complex haplotype determines hsp70-dependent protection against measles virus neurovirulence", *Journal of virology,* vol. 83, no. 11, pp. 5544-5555.

Carsillo, T., Traylor, Z., Choi, C., Niewiesk, S. & Oglesbee, M. 2006, "hsp72, a host determinant of measles virus neurovirulence", *Journal of virology,* vol. 80, no. 22, pp. 11031-11039.

Cattaneo, R. 1994, "Biased (A→ I) hypermutation of animal RNA virus genomes", *Current opinion in genetics & development,* vol. 4, no. 6, pp. 895-900.

Cattaneo, R., Schmid, A., Spielhofer, P., Kaelin, K., Baczko, K., Ter Meulen, V., Pardowitz, J., Flanagan, S., Rima, B.K. & Udem, S.A. 1989, "Mutated and hypermutated genes of persistent measles viruses which caused lethal human brain diseases", *Virology,* vol. 173, no. 2, pp. 415-425.

Childs, K., Andrejeva, J., Randall, R. & Goodbourn, S. 2009, "Mechanism of mda-5 Inhibition by paramyxovirus V proteins", *Journal of virology,* vol. 83, no. 3, pp. 1465-1473.

Chou, S.M. 1986, "Inclusion body myositis: a chronic persistent mumps myositis?", *Human pathology,* vol. 17, no. 8, pp. 765-777.

Chou, S. 1967, "Myxovirus-like structures in a case of human chronic polymyositis", *Science,* vol. 158, no. 3807, pp. 1453-1455.

Connuck, D.M., Sleeper, L.A., Colan, S.D., Cox, G.F., Towbin, J.A., Lowe, A.M., Wilkinson, J.D., Orav, E.J., Cuniberti, L. & Salbert, B.A. 2008, "Characteristics and outcomes of cardiomyopathy in children with Duchenne or Becker muscular dystrophy: a comparative study from the Pediatric Cardiomyopathy Registry", *American Heart Journal,* vol. 155, no. 6, pp. 998-1005.

Cowley, S., Paterson, H., Kemp, P. & Marshall, C.J. 1994, "Activation of MAP kinase kinase is necessary and sufficient for PC12 differentiation and for transformation of NIH 3T3 cells", *Cell,* vol. 77, no. 6, pp. 841-852.

Curran, J., Boeck, R., Lin-Marq, N., Lupas, A. & Kolakofsky, D. 1995, "Paramyxovirus phosphoproteins form homotrimers as determined by an epitope dilution assay, via predicted coiled coils", *Virology,* vol. 214, no. 1, pp. 139-149.

Dabbagh, A., Gacic-Dobo, M., Simons, E., Featherstone, D., Strebel, P., Okwo-Bele, J., Hoekstra, E., Chopra, M., Uzicanin, A. & Cochi, S. 2009, "Global measles mortality, 2000-2008.", *Morbidity and Mortality Weekly Report,* vol. 58, no. 47, pp. 1321-1326.

Dalakas, M.C., Park, K., Semino-Mora, C., Lee, H.S., Sivakumar, K. & Goldfarb, L.G. 2000, "Desmin myopathy, a skeletal myopathy with cardiomyopathy caused by mutations in the desmin gene", *New England Journal of Medicine,* vol. 342, no. 11, pp. 770-780.

Das, T., Gupta, A.K., Sims, P.W., Gelfand, C.A., Jentoft, J.E. & Banerjee, A.K. 1995, "Role of cellular casein kinase II in the function of the phosphoprotein (P) subunit of RNA polymerase of vesicular stomatitis virus", *Journal of Biological Chemistry,* vol. 270, no. 41, pp. 24100-24107.

Devaux, P., von Messling, V., Songsungthong, W., Springfeld, C. & Cattaneo, R. 2007, "Tyrosine 110 in the measles virus phosphoprotein is required to block STAT1 phosphorylation", *Virology,* vol. 360, no. 1, pp. 72-83.

Dobrowolny, G., Aucello, M., Rizzuto, E., Beccafico, S., Mammucari, C., Bonconpagni, S., Belia, S., Wannenes, F., Nicoletti, C. & Del Prete, Z. 2008, "Skeletal Muscle Is a Primary Target of $SOD1^{G93A}$-Mediated Toxicity", *Cell metabolism,* vol. 8, no. 5, pp. 425-436.

Doherty, T.M., Chougnet, C., Schito, M., Patterson, B.K., Fox, C., Shearer, G.M., Englund, G. & Sher, A. 1999, "Infection of HIV-1 transgenic mice with Mycobacterium avium induces the expression of infectious virus selectively from a Mac-1-positive host cell population", *The Journal of Immunology,* vol. 163, no. 3, pp. 1506-1515.

Equils, O., Schito, M.L., Karahashi, H., Madak, Z., Yarali, A., Michelsen, K.S., Sher, A. & Arditi, M. 2003, "Toll-like receptor 2 (TLR2) and TLR9 signaling results in HIV-long terminal repeat trans-activation and HIV replication in HIV-1 transgenic mouse spleen cells: implications of simultaneous activation of TLRs on HIV replication", *The Journal of Immunology,* vol. 170, no. 10, pp. 5159-5164.

Fooks, A.R., Stephenson, J.R., Warnes, A., Dowsett, A.B., Rima, B.K. & Wilkinson, G.W. 1993, "Measles virus nucleocapsid protein expressed in insect cells assembles into nucleocapsid-like structures", *Journal of general virology,* vol. 74, pp. 1439-1444.

Gannagé, M., Dormann, D., Albrecht, R., Dengjel, J., Torossi, T., Rämer, P.C., Lee, M., Strowig, T., Arrey, F. & Conenello, G. 2009, "Matrix protein 2 of influenza A virus blocks autophagosome fusion with lysosomes", *Cell host & microbe,* vol. 6, no. 4, pp. 367-380.

Garg, R.K. 2008, "Subacute sclerosing panencephalitis", *Journal of neurology,* vol. 255, no. 12, pp. 1861-1871.

Gazzinelli, R.T., Sher, A., Cheever, A., Gerstberger, S., Martin, M.A. & Dickie, P. 1996, "Infection of human immunodeficiency virus 1 transgenic mice with Toxoplasma gondii stimulates proviral transcription in macrophages in vivo.", *The Journal of experimental medicine,* vol. 183, no. 4, pp. 1645-1655.

Gemma, T., Watari, T., Akiyama, K., Miyashita, N., Shin, Y., Iwatsuki, K., Kai, C. & Mikami, T. 1996, "Epidemiological observations on recent outbreaks of canine distemper in Tokyo area.", *The Journal of veterinary medical science/the Japanese Society of Veterinary Science,* vol. 58, no. 6, pp. 547.

Giraudon, P., Ch, G. & Wild, T. 1984, "A study of measles virus antigens in acutely and persistently infected cells using monoclonal antibodies: differences in the accumulation of certain viral proteins", *Intervirology,* vol. 21, no. 2, pp. 110-120.

González-Scarano, F. & Rima, B. 1999, "Infectious etiology in multiple sclerosis: the debate continues", *Trends in microbiology,* vol. 7, no. 12, pp. 475-477.

Griffin, D.E. 2007, *Fields Virology,* 5th edn, Lippincott Williams & Wilkins, Philadelphia.

Guidotti, L.G., Matzke, B., Schaller, H. & Chisari, F.V. 1995, "High-level hepatitis B virus replication

in transgenic mice.", *Journal of virology,* vol. 69, no. 10, pp. 6158-6169.

Haas, L., Martens, W., Greiser-Wilke, I., Mamaev, L., Butina, T., Maack, D. & Barrett, T. 1997, "Analysis of the haemagglutinin gene of current wild-type canine distemper virus isolates from Germany", *Virus research,* vol. 48, no. 2, pp. 165-171.

Hara, T., Nakamura, K., Matsui, M., Yamamoto, A., Nakahara, Y., Suzuki-Migishima, R., Yokoyama, M., Mishima, K., Saito, I. & Okano, H. 2006, "Suppression of basal autophagy in neural cells causes neurodegenerative disease in mice", *Nature,* vol. 441, no. 7095, pp. 885-889.

Harder, T.C., Kenter, M., Vos, H., Siebelink, K., Huisman, W., Van Amerongen, G., Örvell, C., Barrett, T., Appel, M. & Osterhaus, A. 1996, "Canine distemper virus from diseased large felids: biological properties and phylogenetic relationships", *Journal of General Virology,* vol. 77, no. 3, pp. 397-405.

Harty, R.N. & Palese, P. 1995, "Measles virus phosphoprotein (P) requires the NH2-and COOH-terminal domains for interactions with the nucleoprotein (N) but only the COOH terminus for interactions with itself", *Journal of General Virology,* vol. 76, no. 11, pp. 2863-2867.

Hashimoto, K., Ono, N., Tatsuo, H., Minagawa, H., Takeda, M., Takeuchi, K. & Yanagi, Y. 2002, "SLAM (CD150)-independent measles virus entry as revealed by recombinant virus expressing green fluorescent protein", *Journal of virology,* vol. 76, no. 13, pp. 6743-6749.

He, C. & Klionsky, D.J. 2009, "Regulation mechanisms and signaling pathways of autophagy", *Annual Review of Genetics,* vol. 43, pp. 67.

Heise, T., Guidotti, L.G., Cavanaugh, V.J. & Chisari, F.V. 1999, "Hepatitis B virus RNA-binding proteins associated with cytokine-induced clearance of viral RNA from the liver of transgenic mice", *Journal of virology,* vol. 73, no. 1, pp. 474-481.

Honda, T., Yoneda, M., Sato, H. & Kai, C. 2013, "Pathogenesis of Encephalitis Caused by Persistent Measles Virus Infection", .

Huber, M., Cattaneo, R., Spielhofer, P., Örvell, C., Norrby, E., Messerli, M., Perriard, J. & Billeter, M.A. 1991, "Measles virus phosphoprotein retains the nucleocapsid protein in the cytoplasm", *Virology,* vol. 185, no. 1, pp. 299-308.

Iwakura, Y., Tosu, M., Yoshida, E., Takiguchi, M., Sato, K., Kitajima, I., Nishioka, K., Yamamoto, K.,

Takeda, T. & Hatanaka, M. 1991, "Induction of inflammatory arthropathy resembling rheumatoid arthritis in mice transgenic for HTLV-I", *Science,* vol. 253, no. 5023, pp. 1026-1028.

Iwasaki, M., Takeda, M., Shirogane, Y., Nakatsu, Y., Nakamura, T. & Yanagi, Y. 2009, "The matrix protein of measles virus regulates viral RNA synthesis and assembly by interacting with the nucleocapsid protein", *Journal of virology,* vol. 83, no. 20, pp. 10374-10383.

Iwatsuki, K., Miyashita, N., Yoshida, E., Gemma, T., Shin, Y., Mori, T., Hirayama, N., Kai, C. & Mikami, T. 1997, "Molecular and phylogenetic analyses of the haemagglutinin (H) proteins of field isolates of canine distemper virus from naturally infected dogs.", *Journal of General Virology,* vol. 78, no. 2, pp. 373-380.

Jackson, W.T., Giddings Jr, T.H., Taylor, M.P., Mulinyawe, S., Rabinovitch, M., Kopito, R.R. & Kirkegaard, K. 2005, "Subversion of cellular autophagosomal machinery by RNA viruses", *PLoS biology,* vol. 3, no. 5, pp. e156.

Janssens, J. & Van Broeckhoven, C. 2013, "Pathological mechanisms underlying TDP-43 driven neurodegeneration in FTLD–ALS spectrum disorders", *Human molecular genetics,* vol. 22, no. R1, pp. R77-R87.

Johansson, K., Bourhis, J., Campanacci, V., Cambillau, C., Canard, B. & Longhi, S. 2003, "Crystal structure of the measles virus phosphoprotein domain responsible for the induced folding of the C-terminal domain of the nucleoprotein", *Journal of Biological Chemistry,* vol. 278, no. 45, pp. 44567-44573.

Karosi, T., Kónya, J., Szabó, L.Z., Pytel, J., Jóri, J., Szalmás, A. & Sziklai, I. 2005, "Codetection of Measles Virus and Tumor Necrosis Factor‐Alpha mRNA in Otosclerotic Stapes Footplates", *The Laryngoscope,* vol. 115, no. 7, pp. 1291-1297.

Katayama, Y., Kohso, K., Nishimura, A., Tatsuno, Y., Homma, M. & Hotta, H. 1998, "Detection of measles virus mRNA from autopsied human tissues", *Journal of clinical microbiology,* vol. 36, no. 1, pp. 299-301.

Kawashima, H., Mori, T., Kashiwagi, Y., Takekuma, K., Hoshika, A. & Wakefield, A. 2000, "Detection and sequencing of measles virus from peripheral mononuclear cells from patients with inflammatory bowel disease and autism", *Digestive diseases and sciences,* vol. 45, no. 4, pp. 723-729.

Kirk, J., Zhou, A., McQuaid, S., Cosby, S. & Allen IV. 1991, "Cerebral endothelial cell infection by measles virus in subacute sclerosing panencephalitis: ultrastructural and in situ hybridization evidence", *Neuropathology and applied neurobiology,* vol. 17, no. 4, pp. 289-297.

Komatsu, M. & Ichimura, Y. 2010, "Physiological significance of selective degradation of p62 by autophagy", *FEBS letters,* vol. 584, no. 7, pp. 1374-1378.

Komatsu, M., Waguri, S., Chiba, T., Murata, S., Iwata, J., Tanida, I., Ueno, T., Koike, M., Uchiyama, Y. & Kominami, E. 2006, "Loss of autophagy in the central nervous system causes neurodegeneration in mice", *Nature,* vol. 441, no. 7095, pp. 880-884.

Komatsu, M., Waguri, S., Koike, M., Sou, Y., Ueno, T., Hara, T., Mizushima, N., Iwata, J., Ezaki, J. & Murata, S. 2007, "Homeostatic levels of p62 control cytoplasmic inclusion body formation in autophagy-deficient mice", *Cell,* vol. 131, no. 6, pp. 1149-1163.

Kurihara, N., Hiruma, Y., Yamana, K., Michou, L., Rousseau, C., Morissette, J., Galson, D.L., Teramachi, J., Zhou, H. & Dempster, D.W. 2011, "Contributions of the Measles Virus Nucleocapsid Gene and the SQSTM1/p62^{P392}Mutation to Paget's Disease", *Cell metabolism,* vol. 13, no. 1, pp. 23-34.

Kurihara, N., Reddy, S.V., Menaa, C., Anderson, D. & Roodman, G.D. 2000, "Osteoclasts expressing the measles virus nucleocapsid gene display a pagetic phenotype", *Journal of Clinical Investigation,* vol. 105, no. 5, pp. 607-614.

Kwong, L.K., Neumann, M., Sampathu, D.M., Lee, V.M. & Trojanowski, J.Q. 2007, "TDP-43 proteinopathy: the neuropathology underlying major forms of sporadic and familial frontotemporal lobar degeneration and motor neuron disease", *Acta Neuropathologica,* vol. 114, no. 1, pp. 63-70.

Kyei, G.B., Dinkins, C., Davis, A.S., Roberts, E., Singh, S.B., Dong, C., Wu, L., Kominami, E., Ueno, T. & Yamamoto, A. 2009, "Autophagy pathway intersects with HIV-1 biosynthesis and regulates viral yields in macrophages", *The Journal of cell biology,* vol. 186, no. 2, pp. 255-268.

Laine, D., Trescol-Biémont, M., Longhi, S., Libeau, G., Marie, J.C., Vidalain, P., Azocar, O., Diallo, A., Canard, B. & Rabourdin-Combe, C. 2003, "Measles virus (MV) nucleoprotein binds to a novel cell surface receptor distinct from FcγRII via its C-terminal domain: role in MV-induced immunosuppression", *Journal of virology,* vol. 77, no. 21, pp. 11332-11346.

Leach, R.J., Singer, F.R., Ench, Y., Wisdom, J.H., Pina, D.S. & Johnson‐Pais, T.L. 2006, "Clinical and cellular phenotypes associated with sequestosome 1 (SQSTM1) mutations", *Journal of Bone and Mineral Research,* vol. 21, no. S2, pp. P45-P50.

Lee, J., Li, Q., Lee, J., Lee, S., Jeong, J.H., Lee, H., Chang, H., Zhou, F., Gao, S. & Liang, C. 2009, "FLIP-mediated autophagy regulation in cell death control", *Nature cell biology,* vol. 11, no. 11, pp. 1355-1362.

Leonard, V.H., Hodge, G., Reyes-del Valle, J., McChesney, M.B. & Cattaneo, R. 2010, "Measles virus selectively blind to signaling lymphocytic activation molecule (SLAM; CD150) is attenuated and induces strong adaptive immune responses in rhesus monkeys", *Journal of virology,* vol. 84, no. 7, pp. 3413-3420.

Levine, B. & Deretic, V. 2007, "Unveiling the roles of autophagy in innate and adaptive immunity", *Nature Reviews Immunology,* vol. 7, no. 10, pp. 767-777.

Levine, B. & Kroemer, G. 2008, "Autophagy in the pathogenesis of disease", *Cell,* vol. 132, no. 1, pp. 27-42.

Lewandowska, E., Lechowicz, W., Szpak, G.M. & Sobczyk, W. 2001, "Quantitative evaluation of intranuclear inclusions in SSPE: correlation with disease duration", *Folia neuropathologica / Association of Polish Neuropathologists and Medical Research Centre, Polish Academy of Sciences,* vol. 39, no. 4, pp. 237-241.

Liebert, U.G., Baczko, K., Budka, H. & Ter Meulen, V. 1986, "Restricted expression of measles virus proteins in brains from cases of subacute sclerosing panencephalitis", *Journal of general virology,* vol. 67, no. 11, pp. 2435-2444.

Longhi, S., Receveur-Bréchot, V., Karlin, D., Johansson, K., Darbon, H., Bhella, D., Yeo, R., Finet, S. & Canard, B. 2003, "The C-terminal domain of the measles virus nucleoprotein is intrinsically disordered and folds upon binding to the C-terminal moiety of the phosphoprotein", *Journal of Biological Chemistry,* vol. 278, no. 20, pp. 18638-18648.

Mamaev, L., Denikina, N., Belikov, S., Volchkov, V., Visser, I., Fleming, M., Kai, C., Harder, T., Liess, B. & Osterhaus, A. 1995, "Characterisation of morbilliviruses isolated from Lake Baikal seals (*Phoca sibirica*)", *Veterinary microbiology,* vol. 44, no. 2, pp. 251-259.

Mammucari, C., Milan, G., Romanello, V., Masiero, E., Rudolf, R., Del Piccolo, P., Burden, S.J., Di Lisi, R., Sandri, C. & Zhao, J. 2007, "FoxO3 controls autophagy in skeletal muscle in vivo", *Cell metabolism,* vol. 6, no. 6, pp. 458-471.

Masuda, M., Sato, H., Kamata, H., Katsuo, T., Takenaka, A., Miura, R., Yoneda, M., Tsukiyama-Kohara, K., Mizumoto, K. & Kai, C. 2006, "Characterization of monoclonal antibodies directed against the canine distemper virus nucleocapsid protein", *Comparative immunology, microbiology and infectious diseases,* vol. 29, no. 2, pp. 157-165.

Mawrin, C., Lins, H., Koenig, B., Heinrichs, T., Murayama, S., Kirches, E., Boltze, C. & Dietzmann, K. 2002, "Spatial and temporal disease progression of adult-onset subacute sclerosing panencephalitis", *Neurology,* vol. 58, no. 10, pp. 1568-1571.

McKenna, M.J. & Mills, B.G. 1989, "Ultrastructural and immunohistochemical evidence of measles virus in active otosclerosis", *Acta Oto-Laryngologica,* vol. 108, no. s470, pp. 130-140.

McQuaid, S., Allen, I., McMahon, J. & Kirk, J. 1994, "Association of measles virus with neurofibrillary tangles in subacute sclerosing panencephalitis: a combined in situ hybridization and immunocytochemical investigation", *Neuropathology and applied neurobiology,* vol. 20, no. 2, pp. 103-110.

McQuaid, S., McMahon, J., Herron, B. & Cosby, S. 1997, "Apoptosis in measles virus‐infected human central nervous system tissues", *Neuropathology and applied neurobiology,* vol. 23, no. 3, pp. 218-224.

Mizushima, N. & Levine, B. 2010, "Autophagy in mammalian development and differentiation", *Nature cell biology,* vol. 12, no. 9, pp. 823-830.

Mizushima, N., Levine, B., Cuervo, A.M. & Klionsky, D.J. 2008, "Autophagy fights disease through cellular self-digestion", *Nature,* vol. 451, no. 7182, pp. 1069-1075.

Mizushima, N., Yoshimori, T. & Levine, B. 2010, "Methods in mammalian autophagy research", *Cell,* vol. 140, no. 3, pp. 313-326.

Morikawa, S., Fukushi, S., Kurane, I., Sakai, K., Ami, K., Yamada, S., Hasegawa, H., Nagata, N., Sata, T. & Matsui, S. 2008, "Outbreak of deadly canine distemper virus infection among imported cynomolgus (crab-eating) monkeys", *IASR,* vol. 29, pp. 315.

Muller, C.P. 2001, "Measles elimination: old and new challenges?", *Vaccine,* vol. 19, no. 17, pp. 2258-2261.

Nakatsu, Y., Ma, X., Seki, F., Suzuki, T., Iwasaki, M., Yanagi, Y., Komase, K. & Takeda, M. 2013, "Intracellular Transport of the Measles Virus Ribonucleoprotein Complex Is Mediated by Rab11A-Positive Recycling Endosomes and Drives Virus Release from the Apical Membrane of Polarized Epithelial Cells", *Journal of virology,* vol. 87, no. 8, pp. 4683-4693.

Nakatsu, Y., Takeda, M., Ohno, S., Shirogane, Y., Iwasaki, M. & Yanagi, Y. 2008, "Measles virus circumvents the host interferon response by different actions of the C and V proteins", *Journal of virology,* vol. 82, no. 17, pp. 8296-8306.

Neumann, M., Sampathu, D.M., Kwong, L.K., Truax, A.C., Micsenyi, M.C., Chou, T.T., Bruce, J., Schuck, T., Grossman, M. & Clark, C.M. 2006, "Ubiquitinated TDP-43 in frontotemporal lobar degeneration and amyotrophic lateral sclerosis", *Science,* vol. 314, no. 5796, pp. 130-133.

Niedermeyer, H., Arnold, W., Neubert, W. & Sedlmeier, R. 2000, "Persistent measles virus infection as a possible cause of otosclerosis: state of the art", *Ear, nose & throat journal,* vol. 79, no. 8, pp. 552-561.

Nishino, I. 2003, "Autophagic vacuolar myopathies", *Current neurology and neuroscience reports,* vol. 3, pp. 64-69.

Niwa, H., Yamamura, K. & Miyazaki, J. 1991, "Efficient selection for high-expression transfectants with a novel eukaryotic vector", *Gene,* vol. 108, no. 2, pp. 193-199.

Noyce, R.S., Bondre, D.G., Ha, M.N., Lin, L., Sisson, G., Tsao, M. & Richardson, C.D. 2011, "Tumor cell marker PVRL4 (nectin 4) is an epithelial cell receptor for measles virus", *PLoS pathogens,* vol. 7, no. 8, pp. e1002240.

Oglesbee, M. 1992, "Intranuclear inclusions in paramyxovirus-induced encephalitis: evidence for altered nuclear body differentiation", *Acta Neuropathologica,* vol. 84, no. 4, pp. 407-415.

Orvedahl, A., Alexander, D., Tallóczy, Z., Sun, Q., Wei, Y., Zhang, W., Burns, D., Leib, D.A. & Levine, B. 2007, "HSV-1 ICP34. 5 confers neurovirulence by targeting the Beclin 1 autophagy protein", *Cell Host & Microbe,* vol. 1, no. 1, pp. 23-35.

Ozanne, G. & d'Halewyn, M. 1992, "Secondary immune response in a vaccinated population during a

large measles epidemic.", *Journal of clinical microbiology,* vol. 30, no. 7, pp. 1778-1782.

Palosaari, H., Parisien, J., Rodriguez, J.J., Ulane, C.M. & Horvath, C.M. 2003, "STAT protein interference and suppression of cytokine signal transduction by measles virus V protein", *Journal of virology,* vol. 77, no. 13, pp. 7635-7644.

Paterson, R.G., Leser, G.P., Shaughnessy, M.A. & Lamb, R.A. 1995, "The paramyxovirus SV5 V protein binds two atoms of zinc and is a structural component of virions", *Virology,* vol. 208, no. 1, pp. 121-131.

Patterson, J.B., Cornu, T.I., Redwine, J., Dales, S., Lewicki, H., Holz, A., Thomas, D., Billeter, M.A. & Oldstone, M. 2001, "Evidence that the hypermutated M protein of a subacute sclerosing panencephalitis measles virus actively contributes to the chronic progressive CNS disease", *Virology,* vol. 291, no. 2, pp. 215-225.

Paula-Barbosa, M., Ruela, C., Faria, R. & Cruz, C. 1980, "Cerebral cortex dendritic degeneration in subacute sclerosing panencephalitis (SSPE)", *Neurology,* vol. 30, no. 1, pp. 7-7.

Perlemuter, G., Sabile, A., Letteron, P., Vona, G., Topilco, A., Chrétien, Y., Koike, K., Pessayre, D., Chapman, J., Barba, G. & Bréchot, C. 2002, "Hepatitis C virus core protein inhibits microsomal triglyceride transfer protein activity and very low density lipoprotein secretion: a model of viral-related steatosis", *The FASEB journal,* vol. 16, no. 2, pp. 185-194.

Pfaller, C.K. & Conzelmann, K. 2008, "Measles virus V protein is a decoy substrate for IκB kinase α and prevents Toll-like receptor 7/9-mediated interferon induction", *Journal of virology,* vol. 82, no. 24, pp. 12365-12373.

Pratakpiriya, W., Seki, F., Otsuki, N., Sakai, K., Fukuhara, H., Katamoto, H., Hirai, T., Maenaka, K., Techangamsuwan, S. & Lan, N.T. 2012, “Nectin4 is an epithelial cell receptor for canine distemper virus and involved in neurovirulence", *Journal of virology,* vol. 86, no. 18, pp. 10207-10210.

Puro, R. & Schneider, R.J. 2007, "Tumor necrosis factor activates a conserved innate antiviral response to hepatitis B virus that destabilizes nucleocapsids and reduces nuclear viral DNA", *Journal of virology,* vol. 81, no. 14, pp. 7351-7362.

Rima, B.K. & Paul Duprex, W. 2005, "Molecular mechanisms of measles virus persistence", *Virus*

research, vol. 111, no. 2, pp. 132-147.

Robbins, S.J. 1983, "Progressive invasion of cell nuclei by measles virus in persistently infected human cells", *Journal of general virology,* vol. 64, no. 10, pp. 2335-2338.

Roelke-Parker, M.E., Munson, L., Packer, C., Kock, R., Cleaveland, S., Carpenter, M., O'Brien, S.J., Pospischil, A., Hofmann-Lehmann, R. & Lutz, H. 1996, "A canine distemper virus epidemic in Serengeti lions (Panthera leo)", *Nature,* vol. 379, no. 6564, pp. 441-445.

Sakai, K., Yoshikawa, T., Seki, F., Fukushi, S., Tahara, M., Nagata, N., Ami, Y., Mizutani, T., Kurane, I. & Yamaguchi, R. 2013, "Canine Distemper Virus Associated with a Lethal Outbreak in Monkeys Can Readily Adapt To Use Human Receptors", *Journal of virology,* vol. 87, no. 12, pp. 7170-7175.

Sandri, M. 2010a, "Autophagy in health and disease. 3. Involvement of autophagy in muscle atrophy", *American Journal of Physiology-Cell Physiology,* vol. 298, no. 6, pp. C1291-C1297.

Sandri, M. 2010b, "Autophagy in skeletal muscle", *FEBS letters,* vol. 584, no. 7, pp. 1411-1416.

Sato, H., Masuda, M., Kanai, M., Tsukiyama-Kohara, K., Yoneda, M. & Kai, C. 2007, "Measles virus N protein inhibits host translation by binding to eIF3-p40", *Journal of virology,* vol. 81, no. 21, pp. 11569-11576.

Sato, H., Masuda, M., Miura, R., Yoneda, M. & Kai, C. 2006, "Morbillivirus nucleoprotein possesses a novel nuclear localization signal and a CRM1-independent nuclear export signal", *Virology,* vol. 352, no. 1, pp. 121-130.

Schaper, J., Froede, R., Hein, S., Buck, A., Hashizume, H., Speiser, B., Friedl, A. & Bleese, N. 1991, "Impairment of the myocardial ultrastructure and changes of the cytoskeleton in dilated cardiomyopathy.", *Circulation,* vol. 83, no. 2, pp. 504-514.

Servant, M.J., Grandvaux, N., Lin, R. & Hiscott, J. 2002, "Recognition of the measles virus nucleocapsid as a mechanism of IRF-3 activation", *Journal of virology,* vol. 76, no. 8, pp. 3659-3669.

Shea, T.B., Fischer, I. & Sapirstein, V.S. 1985, "Effect of retinoic acid on growth and morphological differentiation of mouse NB2a neuroblastoma cells in culture", *Developmental Brain Research,* vol. 21, no. 2, pp. 307-314.

Simons, E., Ferrari, M., Fricks, J., Wannemuehler, K., Anand, A., Burton, A. & Strebel, P. 2012, "Assessment of the 2010 global measles mortality reduction goal: results from 358 a model of surveillance data", *Lancet,* vol. 379, pp. 2173-2178.

Sonoda, S. & Nakayama, T. 2001, "Detection of measles virus genome in lymphocytes from asymptomatic healthy children", *Journal of medical virology,* vol. 65, no. 2, pp. 381-387.

Sun, Z., Li, A., Ye, H., Shi, Y., Hu, Z. & Zeng, L. 2010, "Natural infection with canine distemper virus in hand-feeding Rhesus monkeys in China", *Veterinary microbiology,* vol. 141, no. 3, pp. 374-378.

Tanida, I., Wakabayashi, M., Kanematsu, T., Minematsu-Ikeguchi, N., Sou, Y., Hirata, M., Ueno, T. & Kominami, E. 2006, "Lysosomal turnover of GABARAP-phospholipid conjugate is activated during differentiation of C2C12 cells to myotubes without inactivation of the mTor kinase-signaling pathway", *Autophagy,* vol. 2, no. 4, pp. 264-271.

Tarbouriech, N., Curran, J., Ruigrok, R.W. & Burmeister, W.P. 2000, "Tetrameric coiled coil domain of Sendai virus phosphoprotein", *Nature Structural & Molecular Biology,* vol. 7, no. 9, pp. 777-781.

Tatsuo, H., Ono, N. & Yanagi, Y. 2001, "Morbilliviruses use signaling lymphocyte activation molecules (CD150) as cellular receptors", *Journal of virology,* vol. 75, no. 13, pp. 5842-5850.

Terao-Muto, Y., Yoneda, M., Seki, T., Watanabe, A., Tsukiyama-Kohara, K., Fujita, K. & Kai, C. 2008, "Heparin-like glycosaminoglycans prevent the infection of measles virus in SLAM-negative cell lines", *Antiviral Research,* vol. 80, no. 3, pp. 370-376.

van den Hof, S., Berbers, G.A., de Melker, H.E. & Conyn-van Spaendonck, M.A. 1999, "Sero-epidemiology of measles antibodies in the Netherlands, a cross-sectional study in a national sample and in communities with low vaccine coverage", *Vaccine,* vol. 18, no. 9, pp. 931-940.

Wakefield, A.J., Pittilo, R., Sim, R., Cosby, S., Stephenson, J., Dhillon, A. & Pounder, R. 1993, "Evidence of persistent measles virus infection in Crohn's disease", *Journal of medical virology,* vol. 39, no. 4, pp. 345-353.

Wang, I., Tsai, K. & Shen, C.J. 2013, "Autophagy activation ameliorates neuronal pathogenesis of FTLD-U mice: A new light for treatment of TARDBP/TDP-43 proteinopathies", *Autophagy,* vol. 9, no. 2, pp. 108-109.

Watanabe, A., Yoneda, M., Ikeda, F., Sugai, A., Sato, H. & Kai, C. 2011, "Peroxiredoxin 1 is required for efficient transcription and replication of measles virus", *Journal of virology,* vol. 85, no. 5, pp. 2247-2253.

Watanabe, A., Yoneda, M., Ikeda, F., Terao-Muto, Y., Sato, H. & Kai, C. 2010, "CD147/EMMPRIN acts as a functional entry receptor for measles virus on epithelial cells", *Journal of virology,* vol. 84, no. 9, pp. 4183-4193.

Weber, O., Schlemmer, K., Hartmann, E., Hagelschuer, I., Paessens, A., Graef, E., Deres, K., Goldmann, S., Niewoehner, U. & Stoltefuss, J. 2002, "Inhibition of human hepatitis B virus (HBV) by a novel non-nucleosidic compound in a transgenic mouse model", *Antiviral Research,* vol. 54, no. 2, pp. 69-78.

Yanagi, Y., Hu, H., Seya, T. & Yoshikura, H. 1994, "Measles virus infects mouse fibroblast cell lines, but its multiplication is severely restricted in the absence of CD46", *Archives of Virology,* vol. 138, no. 1-2, pp. 39-53.

Yokota, S., Okabayashi, T., Yokosawa, N. & Fujii, N. 2008, "Measles virus P protein suppresses Toll-like receptor signal through up-regulation of ubiquitin-modifying enzyme A20", *The FASEB Journal,* vol. 22, no. 1, pp. 74-83.

Zeng, M. & Zhou, J. 2008, "Roles of autophagy and mTOR signaling in neuronal differentiation of mouse neuroblastoma cells", *Cellular signalling,* vol. 20, no. 4, pp. 659-665.

Zhang, X., Glendening, C., Linke, H., Parks, C.L., Brooks, C., Udem, S.A. & Oglesbee, M. 2002, "Identification and characterization of a regulatory domain on the carboxyl terminus of the measles virus nucleocapsid protein", *Journal of virology,* vol. 76, no. 17, pp. 8737-8746.

Zhao, J., Brault, J.J., Schild, A., Cao, P., Sandri, M., Schiaffino, S., Lecker, S.H. & Goldberg, A.L. 2007, "FoxO3 coordinately activates protein degradation by the autophagic/lysosomal and proteasomal pathways in atrophying muscle cells", *Cell metabolism,* vol. 6, no. 6, pp. 472-483.

ABSTRACT IN JAPANESE

論 文 の 内 容 の 要 旨

獣 医 学 専 攻
平成22年度博士課程 入学
氏 名 権 賢貞
指導教員名 甲斐 知恵子

論文題目 Analyses of the measles virus inclusion body in muscle and nervous system
（筋肉・神経系における麻疹ウイルス封入体蓄積の影響の解析）

麻疹ウイルス（MV）はパラミクソウイルス科モルビリウイルス属に属する RNA ウイルスで、急性感染時は発熱、発疹、カタル症状、免疫抑制などを引き起こす。急性感染で発症した患者の一部は脳内持続感染により亜急性硬化性全脳炎(SSPE)を引き起こす。SSPE の患者から分離された麻疹ウイルスは変異により感染細胞からのウイルス粒子の放出がほとんど起きない。麻疹ウイルスの封入体は急性感染患者の組織と SSPE 患者の脳組織の両方から観察される。この封入体は麻疹ウイルスを構成するウイルスゲノムおよびタンパクが蓄積されたもので、その中で最もよく検出されるのは麻疹ウイルス N タンパク(MV-N)である。また、無症状のヒトからも MV-N の mRNA が検出された例が報告されているが、この mRNA が実際病原性を持っているかは不明である。本研究では麻疹ウイルス封入体の病理学的意義を調べるために、封入体の主な構成物である MV-N タンパクを発現するトランスジェニックマウスおよび細胞の解析を行った。本論文は以下 3 章より構成される。

第 1 章：MV-N 発現トランスジェニックマウスの作製

麻疹ウイルス封入体の機能を調べるために、遺伝子の全身性発現を誘導する CAG プロモーターの制御下で MV-N を発現するトランスジェニックマウス（MV-N Tg マウス）を作製した。作製の結果、

計 4 匹のファウンダーマウスが生まれ、各マウスの尻尾組織で MV-N mRNA が発現することを確認した。4匹のファウンダーマウスは約8週齢まで正常に成長したが、その後、2 匹のファウンダーマウスから緩慢な体重減少、行動量の減少などの症状が観察された。症状が現れた 2 匹のマウスは約4ケ月齢で死亡した。H-E 染色で死亡マウスの組織を野生型マウスと比べた結果、心筋の変性、平滑筋・骨格筋の萎縮および脾臓の萎縮が観察された。この変化は無症状の MV-N Tg マウスでは観察されなかった。次に免疫組織化学染色法で MV-N の発現を調べた結果、症状のあった 2 匹のマウスでは MV-N の発現が心筋、骨格筋、及び平滑筋に限局されていた。無症状の MV-N Tg マウスでは筋肉系での MV-N 発現が認められなかった。これらの結果から、MV-N の発現が筋肉変性に関与し得ることが示唆された。今まで麻疹ウイルス感染において筋肉系はあまり注目されていなかったが、本実験の結果により無症状のヒトの筋肉組織に存在する MV-N が単独で筋肉変性に関与する可能性が示唆された。

第 2 章:MV-N の筋疾患への影響の解析

第 1 章で作製された MV-N Tg マウスにおいて、MV-N の発現の筋肉変性への影響を解析した。MV-N マウスの骨格筋および心筋は封入体ミオパチーなどの自己貪食空胞性ミオパチーと似た特徴を持っていた。自己貪食空胞性ミオパチーでは筋変性過程にオートファジーが関与することが強く疑われる。筆者はこの点に着目し、免疫組織化学染色法で MV-N Tg マウスの筋肉病変内の各種オートファジー関連分子の分布を調べた。その結果、MV-N Tg マウスの心筋および骨格筋の病変では ubiquitin、p62、LC3 などのオートファジー関連分子が蓄積することが分かった。

次に、MV-N による筋肉変性の機序を調べるためにマウス筋芽細胞株 C2C12 に MV-N を導入し、筋管細胞への分化を誘導した。その結果、MV-N が C2C12 細胞の筋管細胞への分化を阻害することが分かった。この傾向は MV 感染細胞からも確認された。また、MV-N を持続発現する C2C12 細胞でオートファジー関連分子の発現量をウェスタンブロッティングで評価した結果、MV-N 高発現細胞では LC3, p62 の発現量が非常に低下していることが分かった。p62 はオートファジーの選択的分解基質である。RT-PCR で MV-N 高発現細胞で p62 の mRNA 発現が減少しなかったことから、p62 の減少は MV-N 高発現細胞でのオートファジー活性の増加により分解されたと推測された。LC3 もオートファジーの進行により分解されるので、MV-N 高発現細胞での LC3 の発現量減少も持続的なオートファジー活性増加の結果だと考えられた。また p62 に対する蛍光免疫染色を行った結果、C2C12 細胞に筋管細胞への分化を誘導した時、一部の MV-N 持続発現細胞で p62 の凝集が増加した。これらのことから MV-N がオートファジー活性を変化させることにより筋分化を抑制する可能性

が示唆された。MV-N Tg マウスの筋肉病変においてもオートファジー関連分子の蓄積が認められたので、MV-N によるオートファジーの活性変化は筋肉変性にも関わる可能性が高いと考えられる。

第 3 章：MV-N の神経変性への影響の解析

第 1 章で作製した MV-N Tg マウスのうち、無症状だった 2 匹のファウンダーマウスを交配維持し 49 匹のマウスを1年以上飼育した結果、2 匹のマウスから旋回運動を主徴とする神経症状が観察された。免疫組織化学法により発症 MV-N Tg マウスの脳内 MV-N 発現を 9 匹の無症状 MV-N Tg マウスと比べた結果、無症状 MV-N Tg マウスに比べて発症 MV-N Tg マウスでの MV-N 発現が増加したことがわかった。また MAP2、GFAP、TDP-43 に対する免疫染色、Luxol fast blue 染色を行った結果、発症 MV-N Tg マウスの脳における神経細胞の変性、消失、樹状突起の消失、脱髄、および TDP-43 proteinopathy などの病変が観察された。

次に、マウス神経芽細胞腫由来 N2a 細胞の神経突起伸長モデルに MV-N を導入し、その影響を調べた。N2a 細胞にレチノイン酸を添加し、4 日後に蛍光免疫染色で突起伸長率を評価した結果、MV-N 発現 N2a 細胞の突起伸長率は約10%で、MV-N 非発現細胞の40%に比べて著しく低下した。N2a 細胞の神経突起伸長率減少は MV 感染細胞でも確認された。また、ウェスタンブロッティングで N2a 細胞の神経細胞マーカーおよびオートファジー関連分子の発現量変化を評価した結果、MV-N 発現細胞では対照群に比べ神経細胞マーカーの発現量およびオートファジー活性の増加が観察された。神経突起伸長率はオートファジーの抑制または促進時に低下することが知られているので、MV-N 発現細胞でのオートファジー活性増加は神経突起伸長率の低下に関わっていると考えられる。

以上の結果は MV-N の神経変性への関与を示唆している。特に、発症マウスで観察された TDP-43 proteinopathy は筋萎縮性側索硬化症（ALS）や前頭側頭葉変性症(FTLD-U)などの神経変性疾患で報告されたもので、MV 持続感染による神経変性とこれらの疾患の発達機序に共通性があることが推測された。また、MV-N によって阻害される神経突起伸長の阻害は、SSPE などでみられる神経突起損傷の機序に MV-N が直接的に関与しうることも示唆する。

本研究において、MV-N 発現トランスジェニックマウスの作製とその解析により、MV-N 蓄積が筋肉変性および神経変性に関与することを示す結果が得られた。さらに、in vitro で C2C12 細胞および N2a 細胞へ MV-N を導入することにより MV-N が神経系および筋肉系の分化を阻害すること、オートファジー活性を変化させることが分かった。本研究の成果により、発症患者の封入体および無症状

のヒトから検出される MV-N の機能および病原性発現への関与機構に関して新たな知見を与えたと考える。